Chapter 5
Micromachining Techniques for Realization of Three-Dimensional Microelectrode Arrays

Swaminathan Rajaraman

5.1 Introduction

Cellular function and response has been a significant subject of human fascination since time immemorial and a major field of study that has improved understanding of the mechanics of the human body. Specifically the functioning of electrogenic or electrically active cells is of particular interest as these cells control several important physiological functions such as visualization, locomotion, and activities of key organs such as the brain, heart, eyes, ears and the spinal cord. Advances in both engineering (including microelectronics, signal processing, microelectronic and biomedical packaging techniques, and micromachining technologies) and biology (including electrophysiology, neuroscience, cardiology, etc.) have contributed toward a better understanding of this field by introducing instrumentation and devices capable of interfacing with cells and tissue. This chapter summarizes the technological achievements in the development of one such instrument which has been fundamental toward electrical interfacing with biological constructs—three-dimensional microelectrode arrays (3-D MEAs), also called 3-D multielectrode arrays or 3-D micromachined probes. These electrode arrays are utilized in stimulating and recording applications both in vitro (outside the body) and in vivo (within the body) from neural tissue, neural cultures, neuromuscular tissue, cardiac tissue, cardiac cultures, 3-D cocultures of electrically active cells, stem cell cultures, and cultured networks of various electrically active cells (e.g., retinal cells).

If we consider neuroscience as an example area of interest (since most of the tools described in this chapter have a neuroscience focus), most physiological functions controlled by the brain involve a coordinated activity of networks of cells

S. Rajaraman, Ph.D. (✉)
Axion BioSystems Inc., ATDC Bioscience Center at the Georgia Institute of Technology, 1819 Peachtree Road, Suite 350, Atlanta, GA 30309, USA
e-mail: srajaraman@axionbio.com; srajaraman@gatech.edu

M. De Vittorio et al. (eds.), *Nanotechnology and Neuroscience: Nano-electronic, Photonic and Mechanical Neuronal Interfacing*, DOI 10.1007/978-1-4899-8038-0_5,

making it imperative that network activity be studied in addition to single cell activity. Studying such single cell activity has dominated the field for a long time with tools such as wire electrodes, tetrodes, glass micropipette electrodes, and patch clamps [1–4]. In fact to this day, these tools serve the very important function of studying isolated ion channels in a single cell (with high fidelity). These ion channels are responsible for controlling the various signaling pathways in a cell.

Microelectrode arrays (MEAs) can be considered both complimentary and competitive to the tools such as wire electrodes and patch clamps. Network-level activity and *extracellular* measurements can be performed with MEAs, while patch clamps and micropipette electrodes measure *intracellular* electrical signals. Specifically, MEAs are tiny electrodes arranged in a geometrically repeatable fashion either in two dimensions (2-D) or three dimensions (3-D). In some cases additional functionality such as multiplexing circuitry or microfluidic ports are integrated with these electrodes. Research has demonstrated that network-level activity and how "cells talk to one another" are the key to understanding not just the healthy state of various organs (such as the brain and the heart) but also to understanding the various disease states [5–7]. MEAs are tools that enable such an understanding.

Since the 1960s, MEAs have become an invaluable tool for scientific discovery and medical advancement. Because they can actively manipulate and monitor cellular activity at both the single cell and tissue level, these tools provide extraordinary insight into complex neural interactions [8]. Today, first-generation MEAs are used in applications as far ranging as drug screening, biosensing, cardiac pacing, and epilepsy research [9, 10]. For example, MEAs were instrumental in the landmark discovery of spontaneous waves in the developing retina [11]. They have also been used to investigate the role of extracellular stimulation in the suppression of epileptic activity [5, 12] and in the study of novel plasticity mechanisms in cultured neural networks [13–15]. Recently, in a wide variety of tissue and culture preparations, MEAs have shown great promise for drug screening [16, 17]; safety pharmacology [18–20]; biosensing [21, 22]; detection of chemical, biological, and environmental toxins [9, 23]; detection of biohazards and bioterrorism agents [24]; neural prosthetics [25, 26]; and acting as bioelectrodes for measurements of various biopotentials such as electromyographic signals, electrocardiographic signals, and nerve conduction studies [27–29].

Figure 5.1 summarizes the application areas for 2-D and 3-D microelectrode arrays. It can be inferred from the figure, the application space for 3-D MEAs spans a wide variety of areas in life sciences making these tools indispensable for advances in several fields.

This chapter summarizes the advances in the microfabrication technologies used to develop 3-D MEAs. These devices have been fabricated out of traditional substrates such as silicon and glass as well as nontraditional substrates such as parylene, SU-8, various metals, polyimides, etc. A variety of both traditional and nontraditional approaches are enumerated. The focus of the chapter is in the micromachining technological advancements and not the applications that have been developed with MEAs. Readers are referred to the various papers cited in the text for details of the applications that have been developed using these tools.

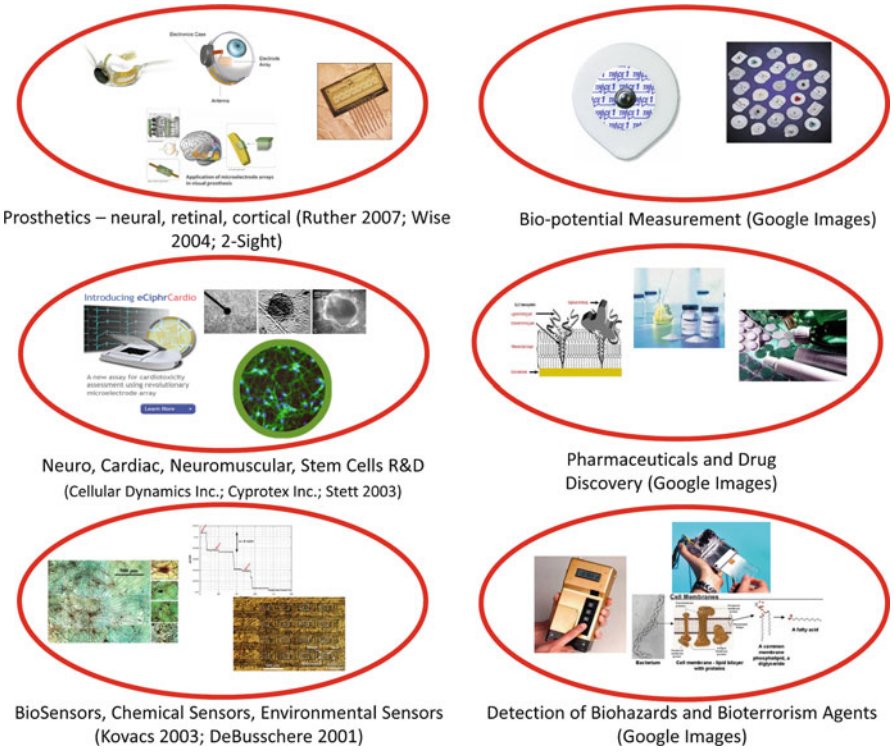

Fig. 5.1 Application space for 3-D MEAs (*top left*, [37], 2-sight) (*center left*, reproduced with permission from [19], © (2003) Springer) (*bottom left*, [23]; reproduced with permission from [24], © (2001) Elsevier)

5.2 Silicon Probes as 3-D MEAs

Prof. Kensall Wise's group at the University of Michigan (Ann Arbor, MI, USA) and Prof. Richard Normann's group at the University of Utah (Salt Lake City, UT, USA) have been at the forefront of 3-D MEAs for in vivo and in vitro applications utilizing silicon probes. Since the introduction of the first integrated circuits (ICs) in the early 1960s, silicon-based technologies have been applied toward biomedical applications. Some of this early work was performed in the development of reading aid for the blind [30], blood flow monitoring [31], and implantable pressure sensors [32].

Silicon-based technologies have been pursued by both the Michigan and Utah groups (and others) due to the several advantages that these technologies have to offer—(a) highly developed microfabrication processes that can produce probes with high yields; (b) batch fabrication on silicon wafers; (c) the ability to create a dense set of microelectrodes that permit acute and semi-chronic single unit and cellular network recordings and stimulation; (d) the ability to be complementary metal-oxide semiconductor (CMOS) compatible for on-chip electronics integration;

(e) the ability to integrate site selection, amplification, and multiplexing circuitry in close proximity to the probe arrays; and (f) the ability to wirelessly transfer information from hundreds of these channels [25].

5.2.1 The Michigan Probes

Prof. Kensall Wise started applying silicon-based technologies toward the creating of thin-film electrodes for single unit recordings in the nervous system when he was a graduate student at Stanford University under the direction of Prof. James Angell in 1966. This microprobe was designed specifically for extracellular biopotential measurement in the brain and consisted of a gold electrode formed on a silicon dioxide (SiO_2) surface, which was defined on a silicon carrier [33, 34]. The insulation in this process was also fabricated from a photolithographically defined layer of SiO_2. Silicon etching which was revolutionary at that time was being used by Bell Telephone Laboratories and was adapted in the original Michigan probe process to define silicon mesas on which the electrodes were defined. The technological achievements of such a process (given that it was performed in the 1960s) are very impressive. From the original silicon wafer (~50 μm), silicon etching was performed to a depth of 25–35 μm on which 2 μm recording sites were defined photolithographically. Figure 5.2 depicts a schematic of a neural probe and an optical image of the first silicon probe as a 3-D MEA and one of the first micromachined arrays that were created anywhere. These probes were utilized in recording extracellular action potentials for the auditory cortex of cats (Fig. 5.3).

This technology was the earliest prototype for a micromachined probe but was not something that could be repeated in a reproducible fashion. Over the next few decades, the development of etch stops, deep reactive-ion etching (DRIE), and anisotropic silicon etching amongst other techniques has created a wide variety of Michigan probes and dramatically advanced this technology. Additionally three-dimensional stacking or assembly technologies were developed to truly fabricate 3-D MEAs with integrated on-chip electronics and wireless data transmission.

Boron diffusion to define etch stops in silicon was one of the key technological breakthroughs that allowed for arbitrary definition of probe thicknesses to less than 15 μm [35, 36]. Conductors such as polysilicon, metal silicides, or metals ranging from gold to tantalum to platinum to iridium are used to define metal tracks and as recording sites in the various Michigan probe microfabrication processes. The choice of the recording site depends on the fabrication process and the charge delivery of the material used. Gold, platinum, and iridium (iridium oxide) are common choices for recording and stimulation sites on the Michigan probes [37].

A combination of silicon dioxide and silicon nitrides deposited utilizing a chemical vapor deposition (CVD) process defined the insulation in this process. The relative proportions of the nitride and oxide in the insulation layer are key to achieving a composite insulator whose thermal expansion coefficient approximately matches that of silicon. This is performed in order to minimize warpage of the structure. Figure 5.4 depicts a very basic fabrication process flow that details the key steps used in the fabrication of the Michigan probes.

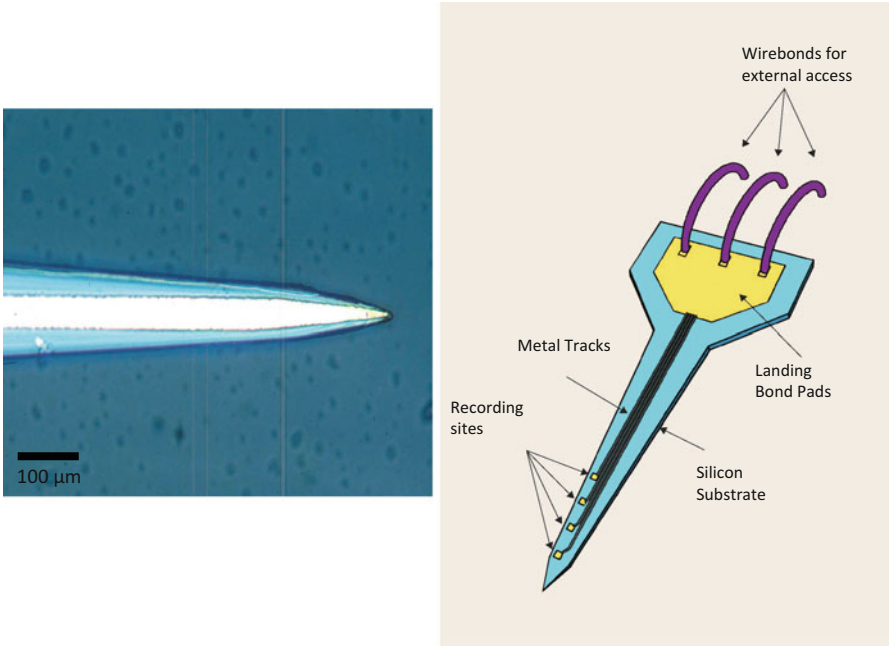

Fig. 5.2 Schematic of a neural probe and the earliest demonstration of a micromachined neural probe (*left*, [25]; *right*, [37])

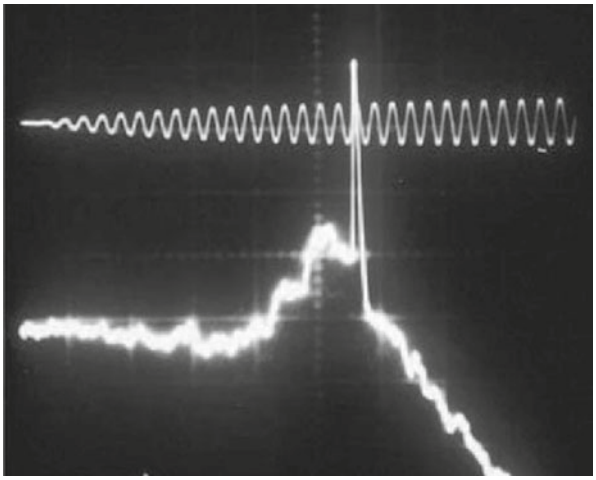

Fig. 5.3 One of the earliest demonstrations of the functioning of a neural probe. Signal recorded from the auditory cortex of a rat [25]

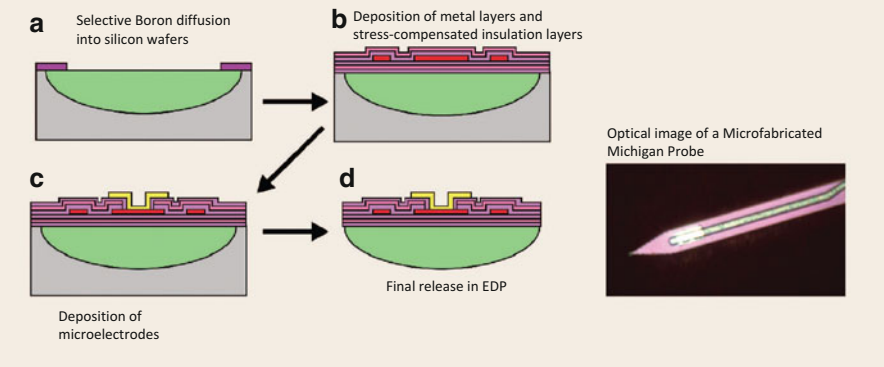

Fig. 5.4 The key steps in the microfabrication of Michigan probes (*left*) and an optical micrograph of a fabricated Michigan probe (*right*) [25]

Ethylenediamine pyrocatechol (EDP) is used as the selective etchant that dissolves the bulk of the wafer and stops at the boron-diffused silicon areas thus serving as the release process for the probes [36–39]. It does not attack any of the other materials used in the microfabrication of the probes. This fabrication technique is versatile to produce arbitrary 2-D probe shapes and site configurations with dimensions controlled to an accuracy of ±1 μm.

In order to fabricate flexible probes for applications such as a cochlear implant, the probe fabrication has been adopted with multiple boron diffusions in specific areas to realize probes that are ultrathin (nanometers) to less than 5 μm in thickness [39, 40].

Both integrated (a CMOS process integrated with the probe fabrication) and hybrid approaches have been taken by Michigan researchers to integrate on-chip circuitry with the probes themselves. A simplified process flow for this CMOS integrated fabrication process flow is depicted schematically in Fig. 5.5. This integrated approach overcomes the external leads issue, which is one of the most difficult problems with any 3-D MEA fabrication, but comes at the expense of a more complicated microfabrication process [37, 41]. Typically a standard CMOS process is first implemented on standard silicon wafers (or silicon-on-insulator (SOI) wafers) with recording/stimulation site metallization performed as one of the last steps in the CMOS fabrication. Finally the field dielectrics are trimmed away, and the silicon in the field area is recessed using a dry etch. The wafer is typically thinned to around 150 μm and then released in EDP. Optical micrographs of Michigan probe arrays with CMOS circuitry are shown in Fig. 5.6. Michigan probe arrays with CMOS circuits are depicted in Fig. 5.7.

In order to develop a truly three-dimensional electrode array with multiple 2-D probe shanks and thousands of recording sites, Michigan researchers have developed several techniques. Some commonalities between these techniques are the integration of a gold beam electroplating process at the end of probe fabrication [42]. These electroplated gold beams are soft enough to be bent with the aid of micromachined assembly devices (which are also constructed on silicon wafers).

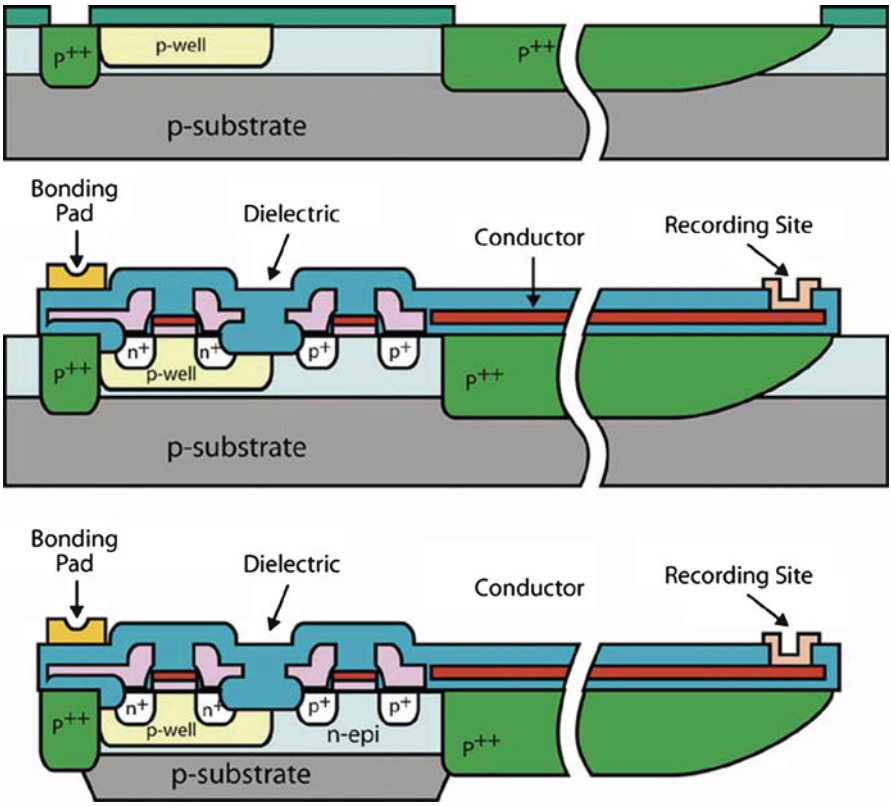

Fig. 5.5 The key steps in a CMOS integrated Michigan probes fabrication process [37]

Ultrasonic wire-free wedge bonding is performed to attach the gold pads of the probe arrays with landing pads of a platform created for assembling multiple probe arrays [43]. Simpler stacking methodologies and more involved dynamic motion-based techniques have been developed to automate this process. Examples of fully assembled 3-D Michigan probe arrays are shown in Fig. 5.8. More recently simple, rapid folding-based techniques have been demonstrated to fabricate 3-D MEAs from planar shanks [44].

The monitoring of electrical activity of the neural network is further enhanced by the ability to monitor and control the chemical "microenvironment" surrounding neural tissue. This first step in achieving such control is adding microfluidics to the Michigan probes. Papageorgiou et al. [45] demonstrate that by adding one mask to the standard Michigan probe fabrication process, microchannels can be created. The combination of a shallow (2 μm deep) unmasked boron etch stop followed by a DRIE step is utilized to create a grid of holes or slots through the etch stop region on top of the intended channel region. The microchannels are then formed utilizing either a dry or wet silicon etch to undercut this grid of slots. The channel access holes are subsequently sealed using a CVD layer of silicon dioxide and silicon nitride. Normal probe process to form interconnects and stimulation/recording sites

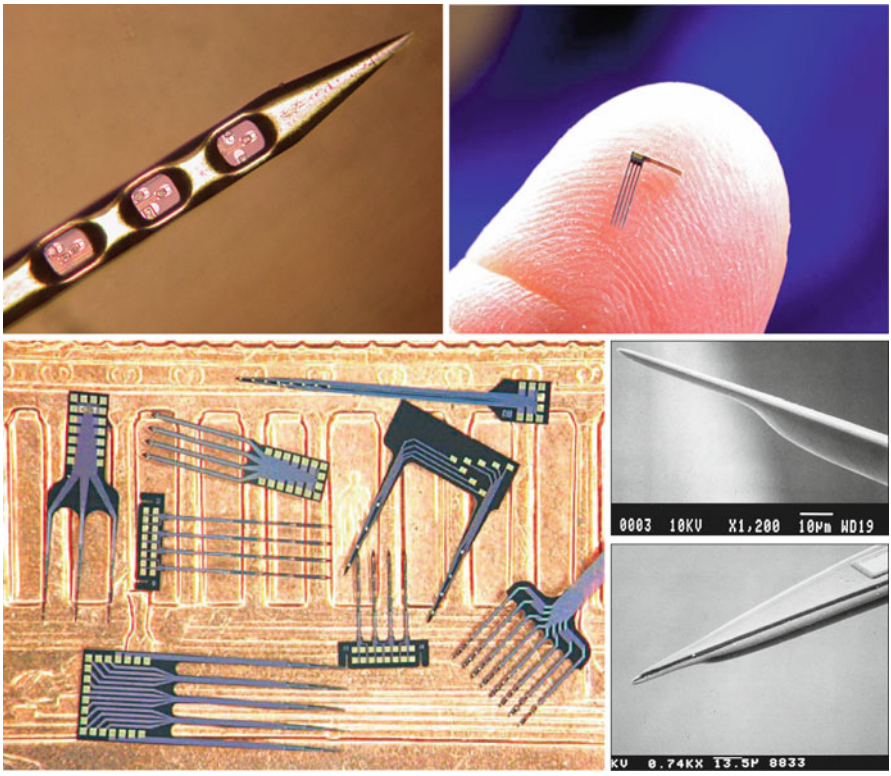

Fig. 5.6 Optical micrographs of fabricated Michigan probes without CMOS circuits integrated. SEM images of single unit probes. *Bottom right* and *top left*, [37], *bottom left*, [25], *top right*, [44]

occur afterward. Figure 5.9 depicts a schematic of Michigan probe arrays with integrated microfluidics and SEM images of probes with such channels.

Michigan probe arrays are well characterized for in vivo applications including retinal prosthesis, cochlear implants, and fundamental neural interfacing studies. The probe fabrication process has proved widely successful providing over 7,000 arrays (up until 2004) to researchers worldwide resulting in over 350 publications [25]. NeuroNexus has commercialized the Michigan probe array process and cites roughly 1,000 publications (from 2005 to 2013) where their probes have been utilized [46]. Figure 5.10 presents a few examples of the data (from the paper references in this chapter) collected from the Michigan probe arrays, which have been used exhaustively in cochlear implants and neural prosthetic applications.

5.2.2 The Utah Array

The first reported microfabrication processing details for the now well-established Utah Electrode Array (UEA) comes from Campbell et al. in 1991 [47]. It reports a

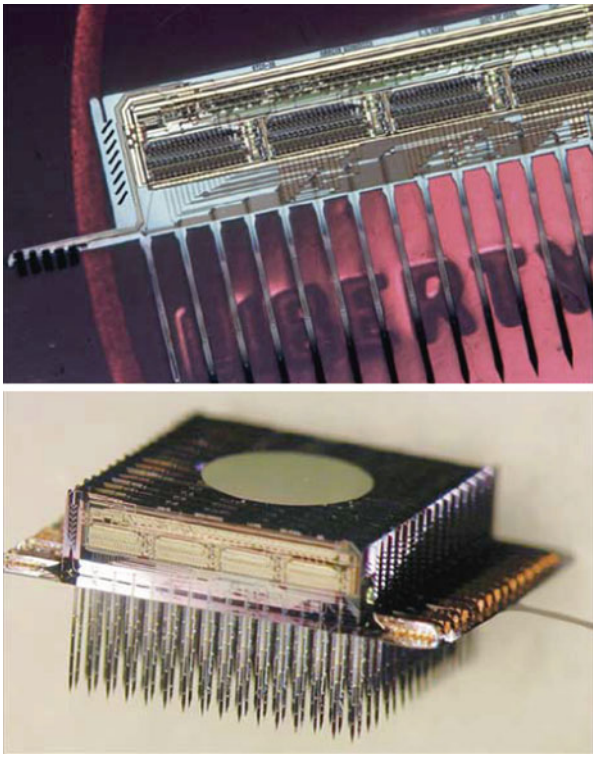

Fig. 5.7 Optical micrographs of CMOS integrated, fully assembled Michigan probes [37]

microfabrication process that has remained remarkably consistent over the years [26] that has the following major steps: (a) thermomigration of p+ silicon into n-type silicon wafers, (b) a combination of mechanical and chemical micromachining to achieve sharp microneedles or 3-D microelectrodes in the p+ silicon areas, (c) metal definition to create active recording sites and contact pads, and (d) encapsulation processes.

The thermomigration process is carried out by defining aluminum pads on the bottom side of a silicon wafer with a lithographic approach. A silicon–aluminum eutectic is driven through the thickness of the wafer with a created temperature gradient [47, 48]. This process creates p+ islands, which are isolated to the region of the aluminum definition and isolated from one another due to the n-type substrate. Aluminum pads are defined for final packaging of the arrays at the bottom of the wafer such that each pad overlaps one island. The nominal design for the Utah array is a 10×10 microneedle structure that is roughly 1–1.5 mm tall. In recent years, up to roughly 8 mm tall needles have been reported with similar processes [49].

In order to create the 3-D microneedles across the thickness of the silicon wafer, a dicing process is used to create hatched grooves in the silicon wafer as

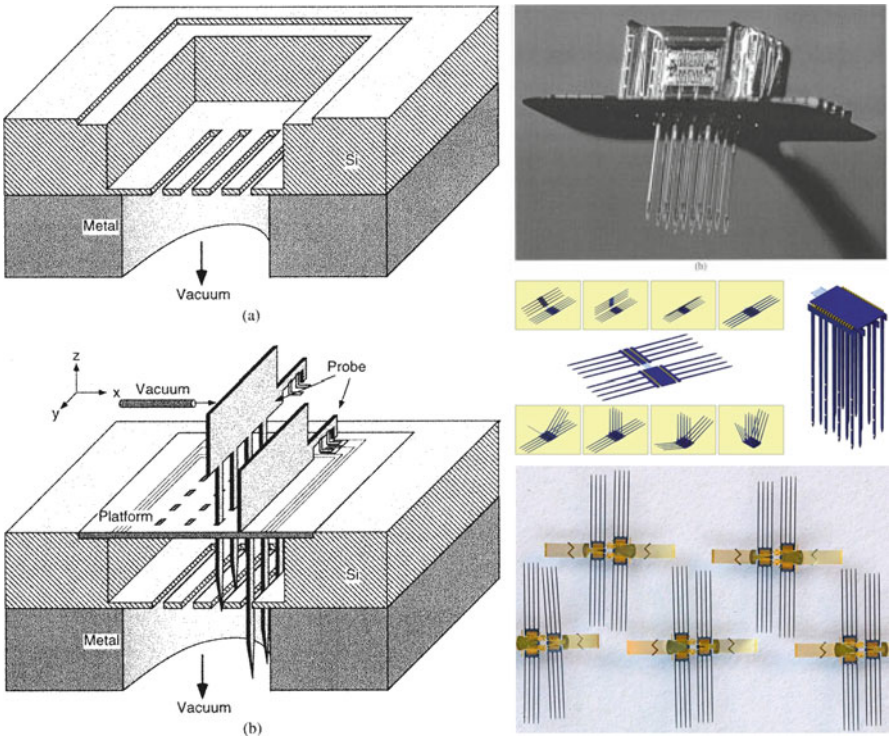

Fig. 5.8 Assembly processes involved in the fabrication of Michigan probes and the resulting assembled probes. *Left* and *top right* [42]; *center right* and *bottom right* [44]

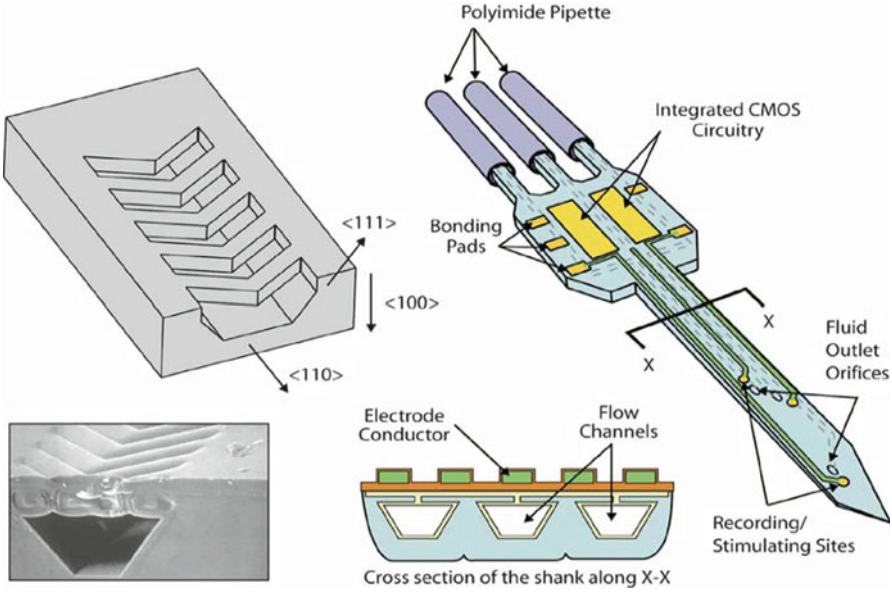

Fig. 5.9 Schematic and SEM images of Michigan probes with integrated microfluidic ports [45]

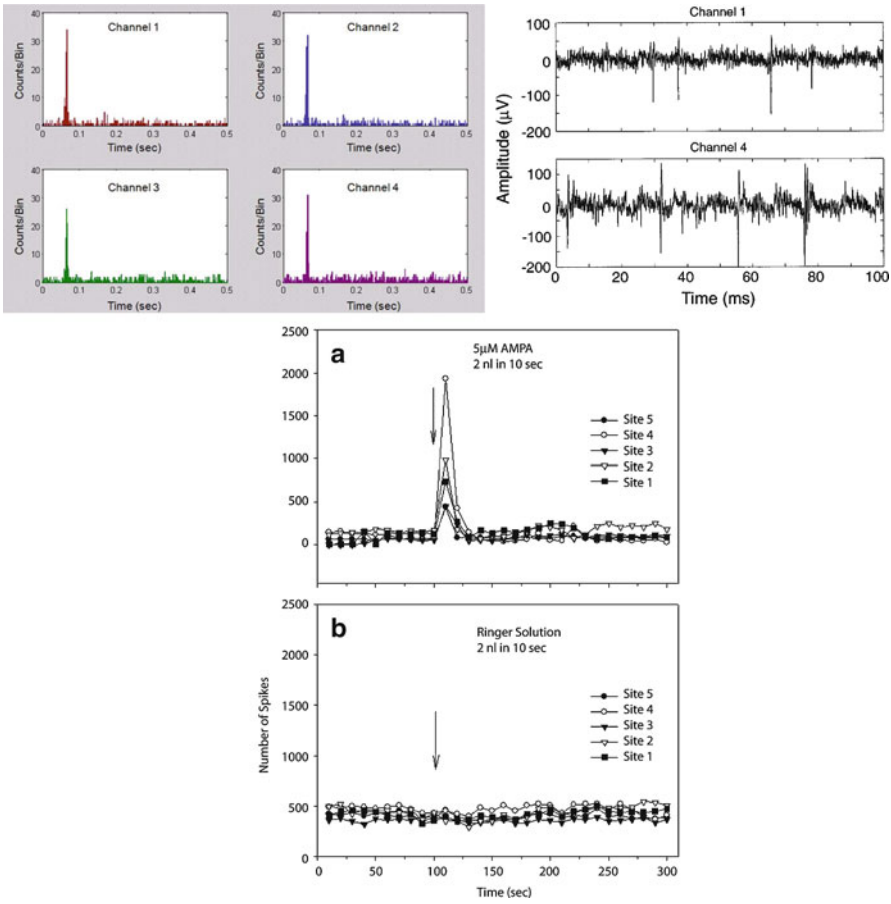

Fig. 5.10 Spike counts on four specific channels on a 3-D array implanted in the auditory cortex of a guinea pig (*top left*); neural discharges from five recording sites in the inferior colliculus of a guinea pig before and after the injection of a neurotransmitter agonist and control (*left*); single unit activity recorded from two different channels from a guinea pig auditory cortex (*top right*). *Top left* [44]; *left* [37]; *top right* [42]

shown in Fig. 5.11. Sometimes a layer of glass is deposited onto these grooves in silicon to effectively isolate the 3-D microelectrodes. Isotropic silicon etching is then carried out in a solution of 5 % hydrofluoric acid (HF) and 95 % nitric acid (HNO_3) [47]. Both static and dynamic modes of etching have been demonstrated to create various shapes and sizes of the silicon microelectrodes as shown in Fig. 5.12.

For the definition of recording sites on the individual 3-D microelectrodes, a couple of techniques are reported—rudimentary metal foil isolation followed by the deposition of gold and platinum in a sputter coater [47, 48] and photoresist masked metal sputtering (metals like gold, platinum, and iridium are reported as recording

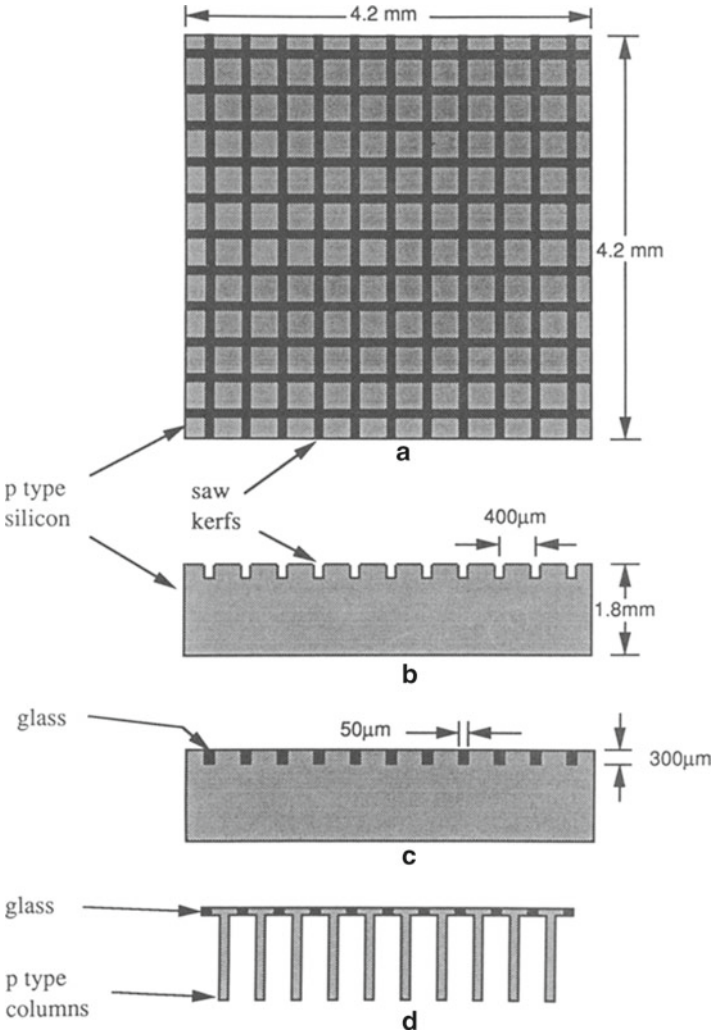

Fig. 5.11 Top and side views of a basic process flow for the Utah array microfabrication process. Reproduced with permission from [48], © (1992) Springer

sites for Utah arrays) followed by the deposition of parylene-C and etching of the parylene layer using a photoresist mask to de-insulate just the tips of the 3-D MEAs [51]. Figure 5.13 illustrates SEM images of the tips of Utah arrays after de-insulation with the techniques described above. Additionally Fig. 5.13 depicts SEM images of Utah arrays with slanted electrodes at various heights.

Encapsulation of the arrays is accomplished using silicon dioxide, silicon nitride, polyimide, and Parylene-C [49, 52]. For de-insulating the tips of the 3-D

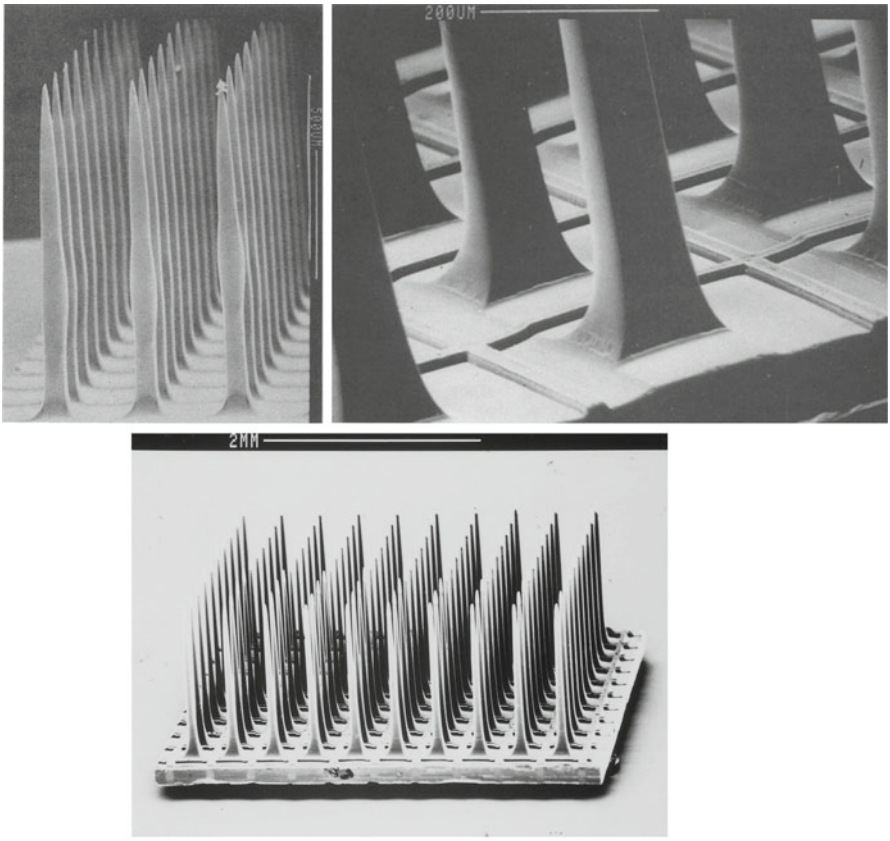

Fig. 5.12 Silicon microneedles of various shapes and sizes created using the Utah array microfabrication process. *Top (right* and *left)*, reproduced with permission from [48] © (1992); *bottom*, reproduced with permission from [50], © (1998) Elsevier

electrodes, rudimentary techniques such as aluminum foil attachment and etching of the polymer in a reactive-ion etch (RIE) to more sophisticated flooding of the array with photoresist with thickness controlled using spin speeds have been demonstrated.

These arrays have been successfully inserted in several studies for neural, retinal, and motion-based prosthetic applications. The Utah array was originally developed as means of restoring limited but useful sight to individuals with profound blindness but has since been applied to produce a sit-to-stand maneuver and other promising prosthetic applications. Figure 5.14 depicts some of these promising applications. Blackrock Microsystems [53] has been able to successfully commercialize this rather complicated process and also provides electronics to interface with these arrays.

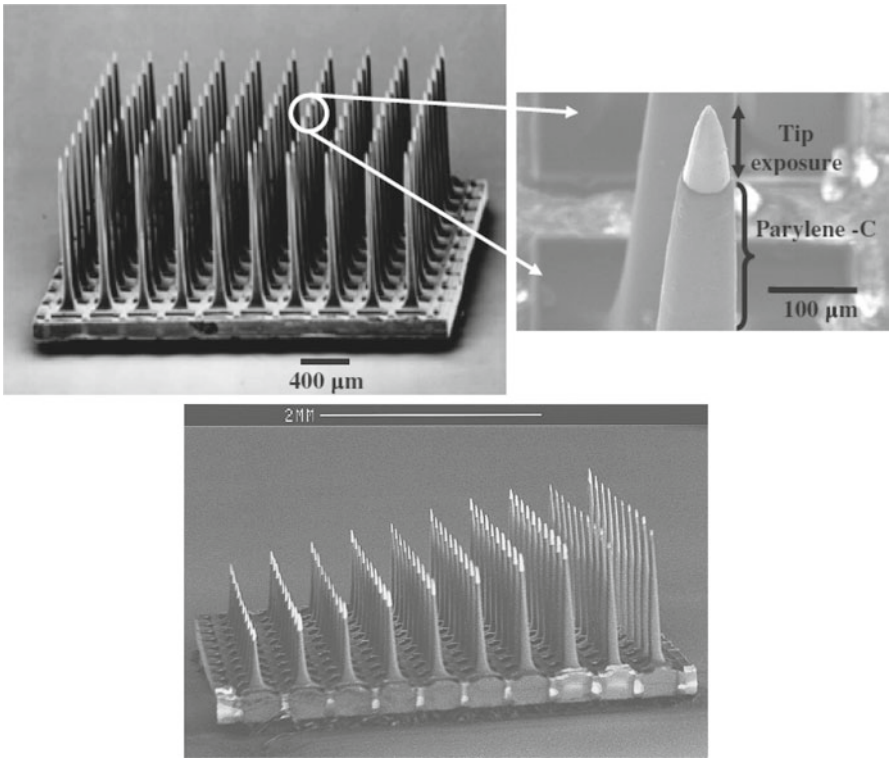

Fig. 5.13 SEM images of the completed Utah array 3-D MEAs. *Top* [51]; *bottom* [54]

5.2.3 EU NeuroProbes

European Union's consortium has been working toward a solution for silicon-based intracortical 3-D microelectrodes. This project is called the European NeuroProbes consortium (www.neuroprobes.org). It was a 4-year integrated project funded by the European Commission with technology development happening in the following institutes: Interuniversity Microelectronics Center (IMEC), Belgium; Department of Microsystems, IMTEK, University of Freiburg, Germany; Hahn-Schickard-Gesellschaft Institute of Micromachining and Information Technology (HSG-IMIT), Germany; Institute of Microtechnology (IMT), University of Neuchatel, Switzerland; and Malardalen University, Sweden [55].

The goal of the EU NeuroProbes effort was to overcome some of the limitations of the Utah arrays and Michigan probes by developing a 3-D implementation of the probe arrays conducive to chronic applications [55] by the development of a platform with emphasis on elegant assembly that would allow for electrode sites for recording and stimulation of cortical neurons, biosensors for monitoring glutamate and dopamine, and integrated microfluidic channels for sampling or drug delivery [56].

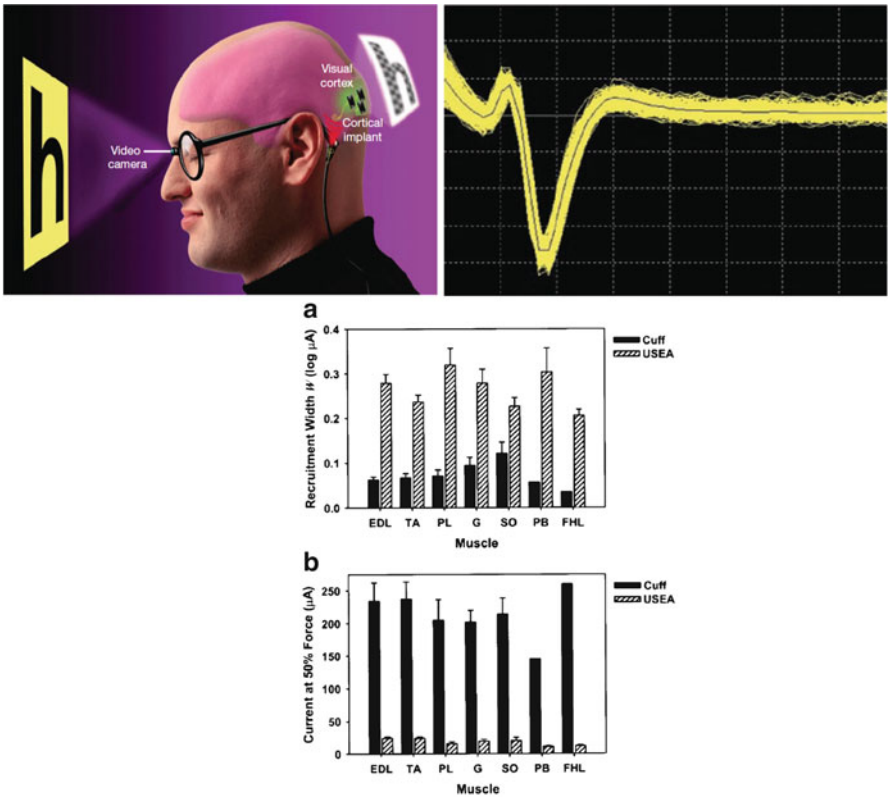

Fig. 5.14 Schematic of a cortex-based artificial vision systems with the Utah array electrodes implanted in the primary visual cortex (*top left* [26]); 285 superimposed recordings of action potentials from a cat's sciatic nerve recorded when the cat's ankle was flexed and extended (*top right* [26]); summary of the recruitment properties of the Utah array and conventional electrodes both measured on the cat sciatic nerve (*bottom* [54])

One of the first papers out of this effort comes from Kisban et al. [57]. This paper describes the fabrication of single-shaft probes with a pitch of 500 μm and lengths of 2, 4, and 8 mm, respectively. To facilitate insertion into the brain tissue, a sharp tip with an opening angle of 17° and a tapered shaft of 0.5°, 0.3°, and 0.1°, respectively, was designed. The thickness of the probes is targeted to be around 120 μm to provide sufficient mechanical stiffness for insertion into brain tissue. Each shaft comprises of eight circular electrodes with a 20 μm diameter and a tip electrode made of platinum. Figure 5.15 represents a basic process flow for these silicon probes. The process starts with the deposition of 500 nm of stress-compensated dielectrics on both sides of a 300 μm-thick silicon wafer. An additional 1.5 μm thick Plasma Enhanced Chemical Vapor Deposition (PECVD) SiO_2 is deposited on the backside of the wafer. The next step is to define metal tracks and the electrodes using a lift-off process. The metal track consists of Ti (30 nm), Au (200 nm), Pt (100 nm), and Ti (30 nm), respectively. The metallization is electrically isolated

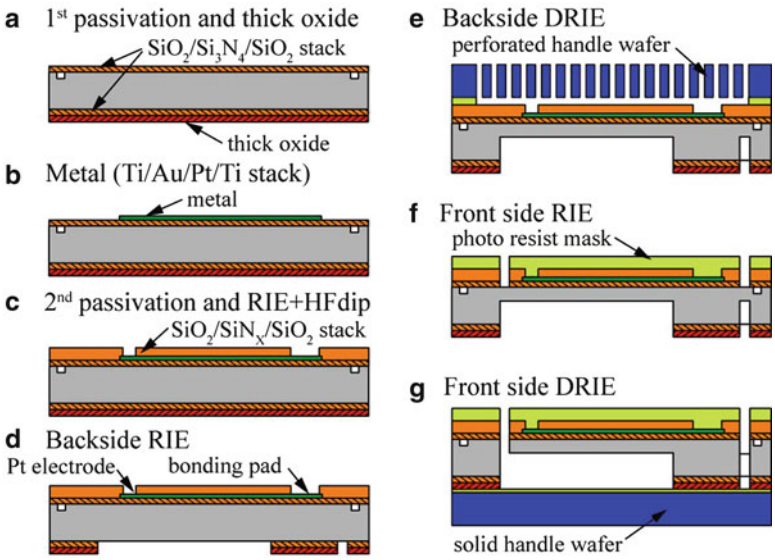

Fig. 5.15 Basic process flow for the EU NeuroProbes approach to the fabrication of silicon 3-D MEAs [57]

with a second stress-compensated PECVD layer, which is defined using an RIE etch and a HF dip. DRIE is now performed from the backside (after an RIE etch of the dielectric layer) to define the probe shaft to its final thickness of around 100 μm. A perforated handle wafer is attached to the front side of the wafer during this process. Front-side processing is performed to release the probe shaft as the final step. This includes removal of the dielectrics with an RIE step and silicon release using a DRIE step. As in the backside-etching step, a handle wafer is used for this step as well. Figure 5.16 depicts optical and SEM images of the silicon probe arrays. A custom ribbon cable is fabricated utilizing two layers of polyimide (PI) with an intermediate layer of metal. The silicon probe array and the PI cable are brought together using a gold bump bonding process (Fig. 5.16). Completed devices are depicted in Fig. 5.17. Herwik et al. [58] describe a variation of this process to include electroplated gold leads for packaging purposes.

Aarts et al. [60] report a *slim-base platform* technology for assembly of the EU NeuroProbes. This technology utilizes a DRIE-etched silicon groove onto which the silicon probes are assembled. Electroplated gold is used as the bonding material between the platform and the probe arrays, which are positioned onto the platform using a flip-chip bonder. Figure 5.18 depicts the schematic, SEM, and optical images of such a platform technology used in assembling the EU NeuroProbes.

Microfluidic ports are integrated with the probes as described by Spieth et al. [62]. Individual probe shafts have an area of $250 \times 250\ \mu m^2$, and this includes a microfluidic channel with a cross section of $50 \times 50\ \mu m^2$. The basic process flow for this integration is depicted in Fig. 5.19. First a two-step DRIE process defines the

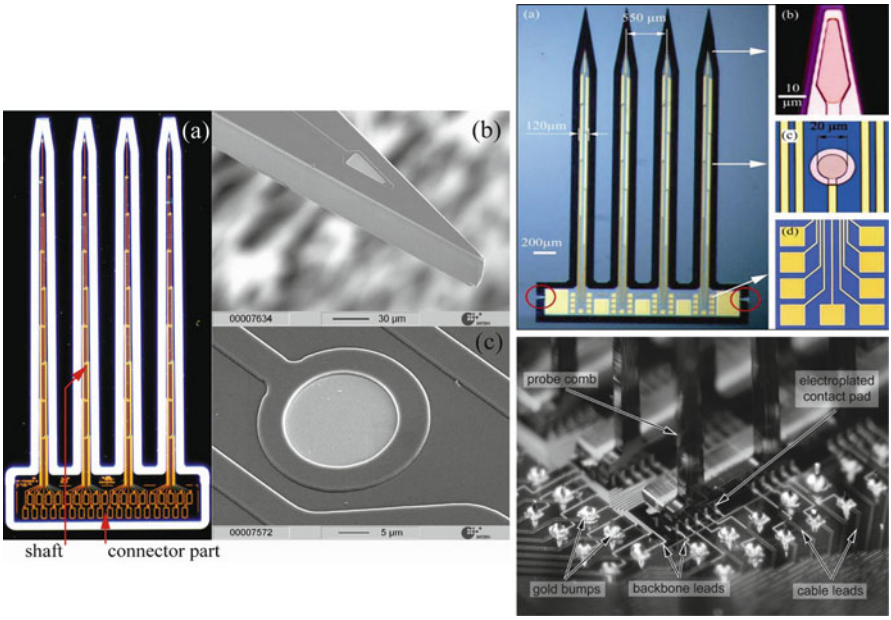

Fig. 5.16 Optical and SEM images of the fabricated probe arrays (*top left* and *right*). Gold bump bonding process for packaging (*bottom right*). *Left* [57]; *top right* [59]; *bottom right*, reproduced with permission from [58], © (2009) IOP Publishing. All Rights reserved

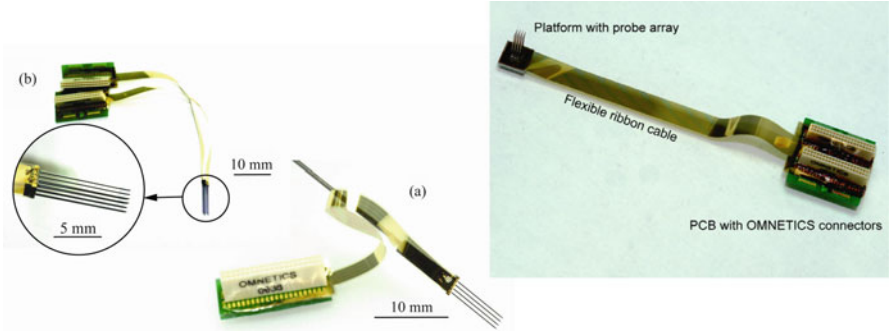

Fig. 5.17 Optical images of assembled probe arrays with flexible polyimide cables. *Left* [57]; *right* [59]

fluidic channel and the outer shape of the probes. The fluidic channel is shaped in the second step with the bonding of a ground silicon wafer. The entire wafer is then passivated on both sides and platinum electrodes are defined. The electrodes are passivated to define the insulation layer and finally thinned down from the bottom side to define a probe shape. Topside silicon etching is also performed to define the fluidic outlet ports. Figure 5.20 depicts SEM images of the constructed devices.

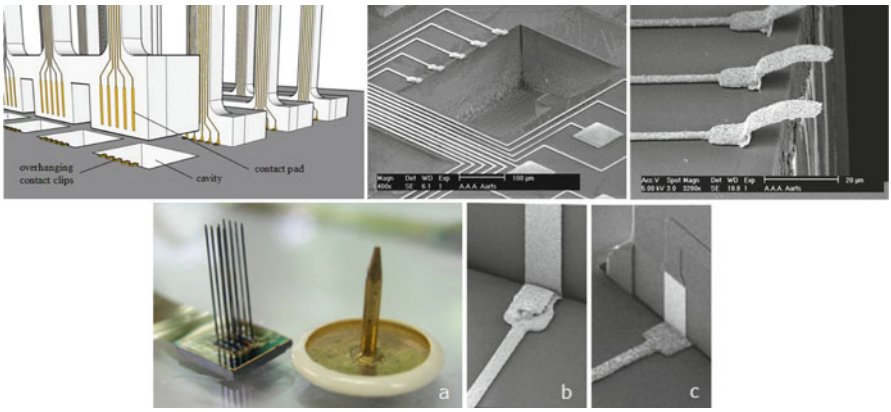

Fig. 5.18 Schematic, optical, and SEM images of assembled probe arrays with a high-throughput assembly technology. *Top left* and *top right* [60], *bottom* [61]

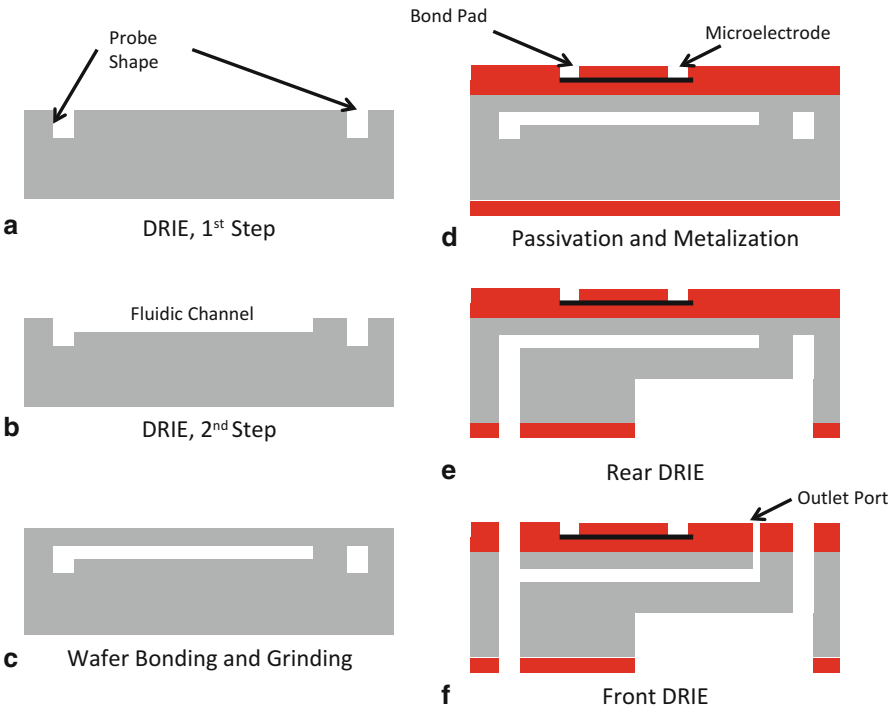

Fig. 5.19 Fabrication process flow to integrate fluidic ports into the EU NeuroProbes. Reproduced with permission from [62], © (2011) Springer

CMOS electronics have been integrated with the EU NeuroProbes as reported by the EU NeuroProbes research team [64, 65]. The *active probe* comprises a 100 µm thick, 4 mm long probe realized using DRIE etching of silicon. It comprises 188 electrodes (20 µm diameter with a pitch of 40 µm) arranged in two columns along

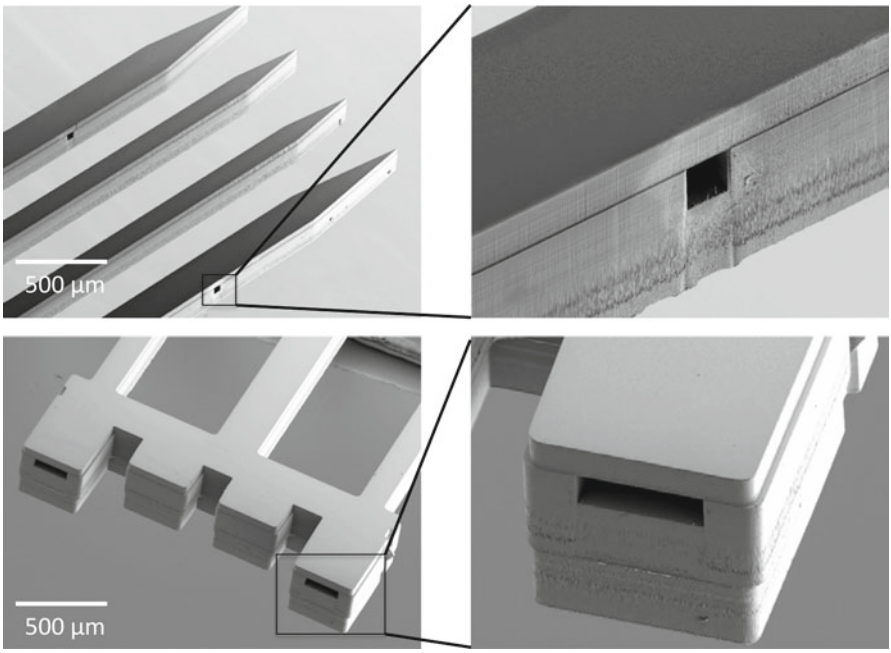

Fig. 5.20 SEM images of EU NeuroProbes with integrated fluidic ports. Reproduced with permission from [63], © (2011) IOP Publishing. All rights reserved

the 4 mm probe. The CMOS circuitry is fabricated as the first step in the construction of these active probes. The post-CMOS fabrication is based on the standard EU NeuroProbes process. The four-mask process for the deposition and patterning of the electrodes, bonding pad metallization and structuring of the probe shafts are depicted in Fig. 5.21. In the first step the passivation layer for the CMOS substrate is opened up to connect to the electrodes and bonding pads realized in post-CMOS metallization. This metallization (300 nm of Pt sandwiched between 30 nm thick Ti adhesion layers) is sputter deposited and patterned using lift-off. Following the post-CMOS metallization, stress-compensated silicon oxide and silicon nitride layer stacks are deposited on both sides of the wafer utilizing a PECVD step. The topside passivation is patterned using RIE etching, and the top Ti layer is wet etched using 1 % Hydrofluoric Acid (HF) to expose the Platinum (Pt) electrodes. The backside passivation is additionally patterned using an RIE process, and the probes are released using DRIE to define a final thickness of 100 µm. A short DRIE step follows from the front side to complete the release of the probes. Figure 5.22 depicts optical micrographs of the *active probe* array.

The EU NeuroProbes project has extended the application platform of this technology for surface electromyography [28] and the integration of amperometric biosensors on the probe shafts for in vivo monitoring of choline and glutamate in the brain [66]. The former uses a suspended etch mask technology which utilizes ICP etching of silicon both anisotropically and isotropically to create microneedles

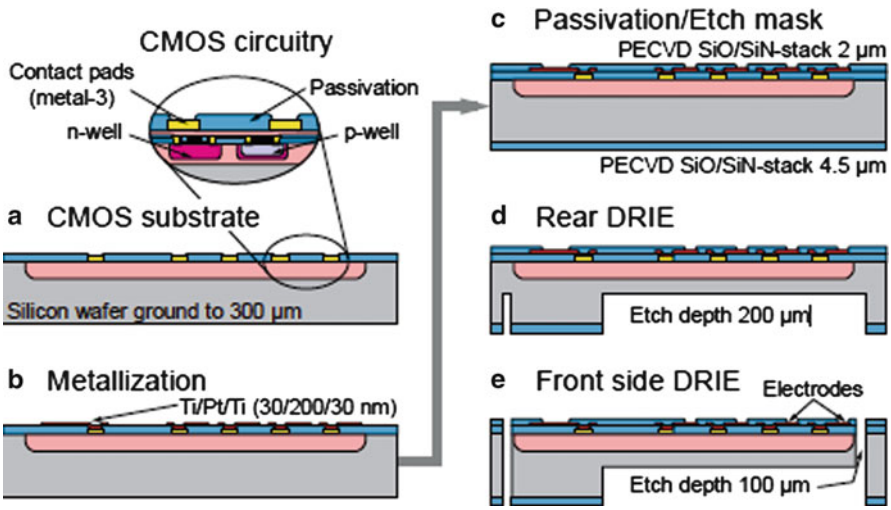

Fig. 5.21 Simplified four-mask process to build EU NeuroProbes on CMOS wafers, using post-CMOS MEMS processing [65]

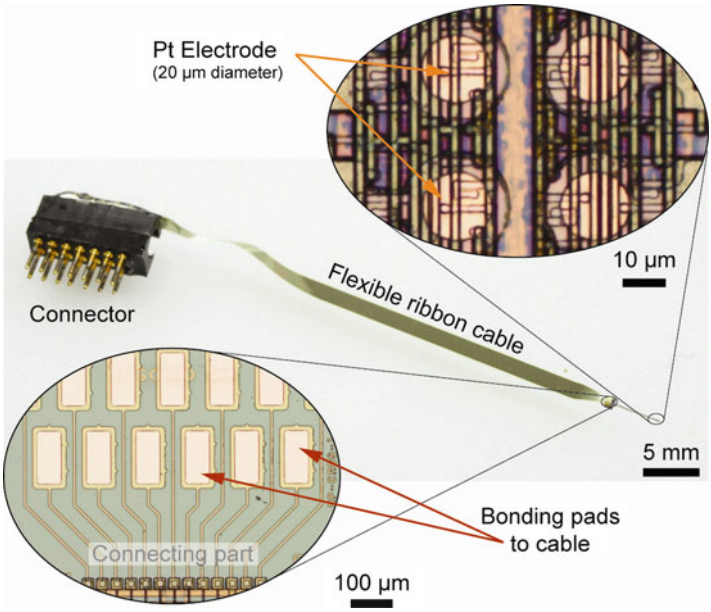

Fig. 5.22 Optical images of an active probe array fabricated using post-CMOS MEMS processing [65]

as depicted in Fig. 5.23. Interconnects are formed utilizing through wafer etching of vias from the backside and metallization (sputter deposition followed by electroplating). The application described by Frey et al. [66] involves the same fabrication process described by Aarts et al. [60] and Herwik et al. [57] which has been

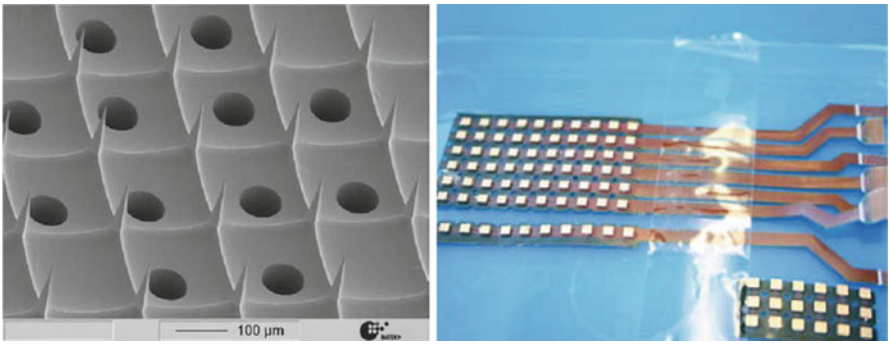

Fig. 5.23 SEM image of the utilization of suspended etch mask technology to create silicon microneedle electrodes (*left*). Packaging these microneedle electrode arrays on a flex circuit (*right*) [28]

described earlier but has a modified probe design. The probe consists of two shanks that are 8 mm in length and have a cross section of 250 µm × 250 µm (height × width). The dimensions of the probe were chosen with the application in mind. Each shank is connected to a common rectangular probe, which comprises the fluidic ports of 25 µm × 50 µm. The shanks comprise five platinum electrodes that are placed around the fluidic ports and have a pitch of 200 µm. The electrodes are 50 µm × 150 µm and are recessed by 10 µm to protect a biosensitive membrane subsequently immobilized on the electrodes. One of the electrodes acts as a reference.

Compared to the Utah arrays and the Michigan probes, both of which have been around for a lot longer than the EU NeuroProbes, the applications developed with these devices are limited but impressive. The in vivo micrograph of the EU NeuroProbes during experimentation and examples of recordings obtained from them are illustrated in Fig. 5.24.

5.2.4 Some Other Major Silicon-Based Approaches

Apart from the three major silicon-based three-dimensional microelectrode array fabrication approaches—Michigan probes, Utah arrays, and EU NeuroProbes—which have been widely published and utilized in a variety of applications, several other researchers have reported other novel silicon-based technologies to fabricate 3-D MEAs. Some of these approaches are briefly described below.

Koo et al. [67] describe a clever utilization of the crystalline structure of silicon to achieve sharp pyramidal tips that have been utilized as 3-D MEAs. In this process the electrode areas on a silicon wafer are first defined using a plasma-enhanced chemical vapor deposition (PECVD) layer of tetraethyl orthosilicate (TEOS) and silicon nitride. Multiple RIE and DRIE steps are carried out with the TEOS and photoresist acting as hard masks to define the vertical dimensions of the 3-D electrodes. Thermal oxidation is then performed to protect the sidewalls of the

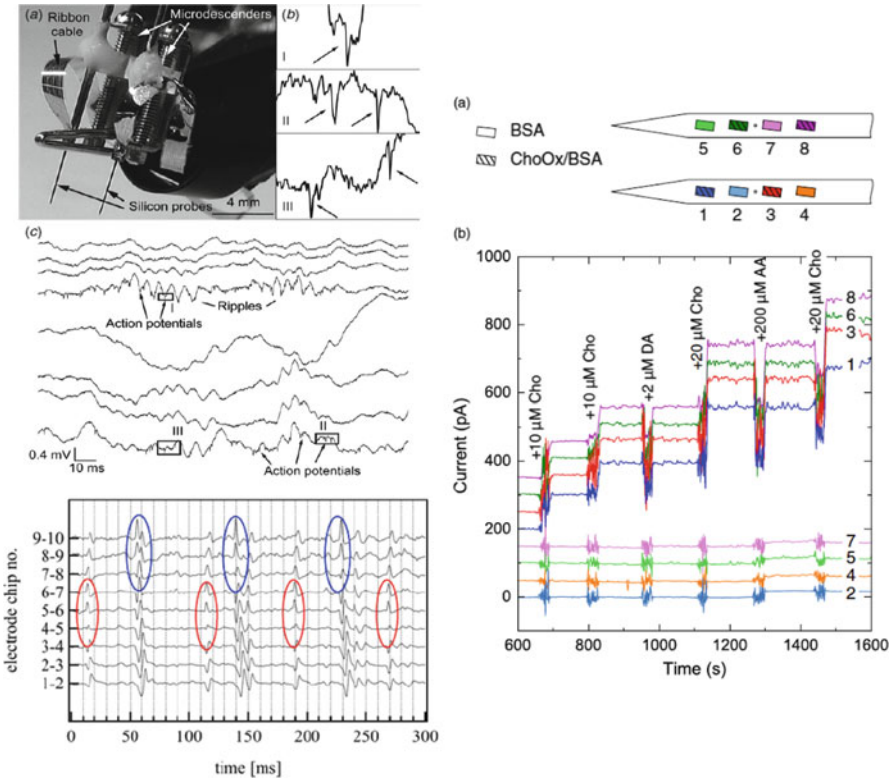

Fig. 5.24 Photograph of the NeuroProbes made ready for implantation and action potentials recorded from individual recording sites in an array (*top left*, reproduced with permission from [58], © (2009) IOP Publishing. All rights reserved); action potentials from regularly firing motor units in the biceps brachii muscle (*bottom* [28]); response of the microprobes to choline and dopamine (*top right*, reproduced with permission from [66], © (2011) IOP Publishing. All rights reserved)

electrodes followed by a potassium hydroxide (KOH) etch to define the 3-D pyramids taking advantage of the fact that the etching stops on the {1 1 1} plane as shown in Fig. 5.25. The electrical pathways are created in the last step after removal of the masking layers (with a 49 % hydrofluoric acid etch) by sputter deposition of a Ti/Au layer and photolithographic definition. The 3-D electrodes are constructed in an 8×8 array roughly 50 µm tall with a 120 µm pitch between electrodes.

Kusko et al. [68] report the fabrication of a 5×5 array of 3-D microelectrodes by the definition of a silicon dioxide/photoresist mask that is carefully undercut by silicon etching—a combination of wet and dry etching—DRIE process to define micropillars first followed by a KOH sharpening to achieve pyramidal tips and DRIE followed by an isotropic silicon etch to create conical tips. The contact metallization and recording sites are then defined by lift-off techniques on 3-D electrodes followed by the deposition of a PECVD silicon dioxide layer and definition of the

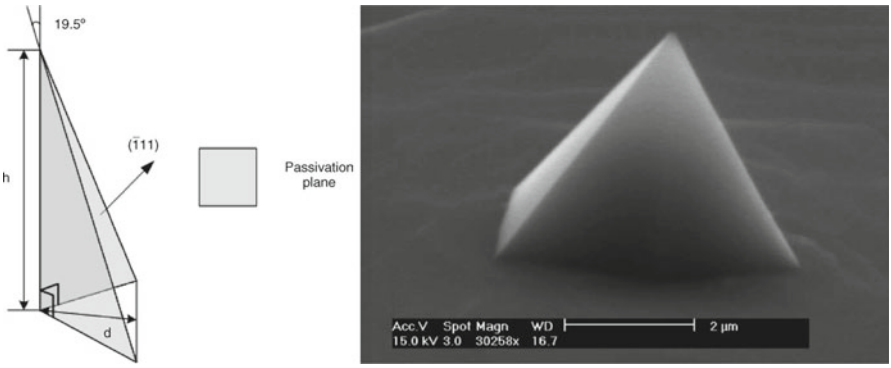

Fig. 5.25 Schematic of the passivation plane where the silicon etching stops (*left*) and SEM image of the defined single microneedle electrode (*right*). Reproduced with permission from [67], © (2006) Elsevier

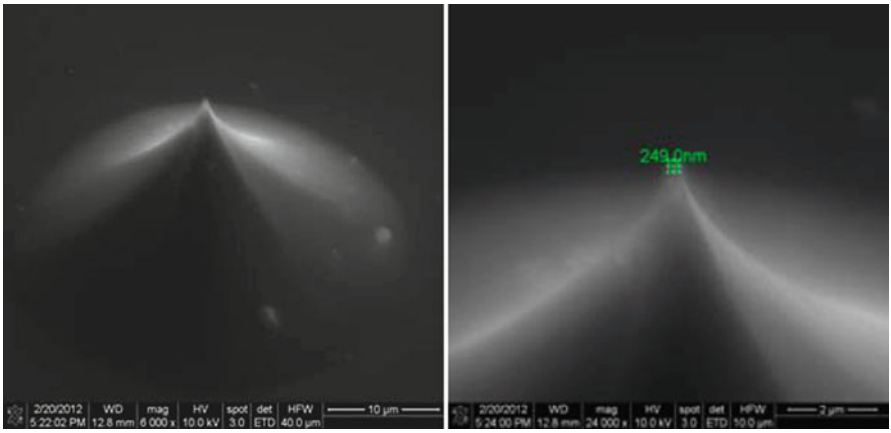

Fig. 5.26 Combination of wet and dry silicon etching to undercut a silicon dioxide/photoresist mask to achieve really sharp nanometer scale tips for 3-D microelectrodes [68]

recording sites lithographically. Three-dimensional microelectrodes that are ~35 µm tall with singular microelectrode tip sharpness of less than 500 nm are achieved using this process as shown in Fig. 5.26.

Du et al. [69] describe a silicon-based process where they utilize double-side thin silicon wafer processing and a carrier wafer to get around handling fragile wafers. So instead of an etch stop used in the Michigan probe approach, this approach uses a 25–50 µm silicon substrates as starting point for MEA fabrication. A 500 µm thick silicon or Pyrex or quartz wafer is used as the carrier in this process. The ultrathin silicon substrate is mounted on the carrier wafer, and metal is defined using a lift-off process. For insulation a 2 µm thick parylene layer is conformally deposited (room temperature vapor deposition process) and defined using

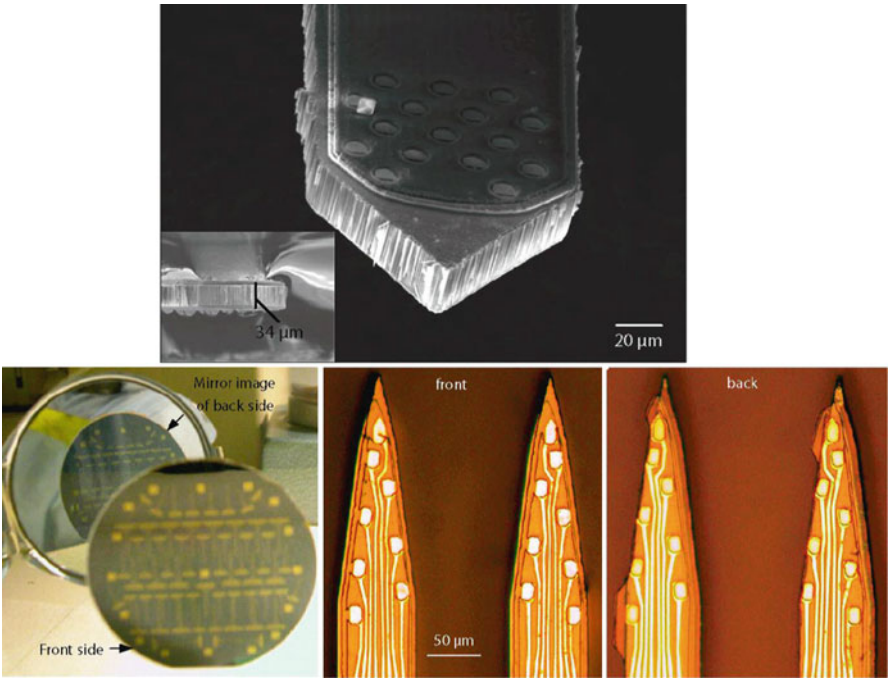

Fig. 5.27 Silicon probes fabricated with the utilization of ultrathin silicon wafers and performing double-side fabrication. Reproduced with permission from [69], © (2009) IOP Publishing. All rights reserved

photolithography and RIE etching. Additionally this approach lends itself to the fabrication of identical probes on both sides of the ultrathin silicon wafers. Probes fabricated utilizing this approach are depicted in Fig. 5.27.

Hanein et al. [70] describe an interesting DRIE etching followed by RIE sharpening and interfacing with a polyimide flex circuit-based approach for the fabrication of intracellular 3-D MEAs. They utilize highly conductive p-type silicon wafers and fabricate protection pillars around 3-D electrodes in the DRIE step. These protection pillars completely etch away during the isotropic RIE sharpening process (utilizing a SF_6 plasma) leaving behind ~230 µm-tall 3-D microelectrodes that are electrically routed using a flex circuit. Figure 5.28 depicts SEM images of the protection pillars with the central 3-D electrode after the etching steps. These are completely etched away leaving behind sharp (~200 nm tips) 3-D microelectrode.

Chu et al. [71] create 3-D MEAs on SOI wafers of various thicknesses by defining the microelectrodes on the device layer first, followed by ICP etching of silicon to create micropillars which are then sharpened by either a dry, isotropic XeF_2 etch or a wet isotropic Hydrofluoric Acid/Nitric Acid/Acetic Acid (HNA) etch. The metal traces are protected during the entire process, which can prove to be difficult. Thermally grown SiO_2 acts as the insulation, and it is removed on the bond pads and the top of the 3-D electrodes by a carefully controlled wet etch.

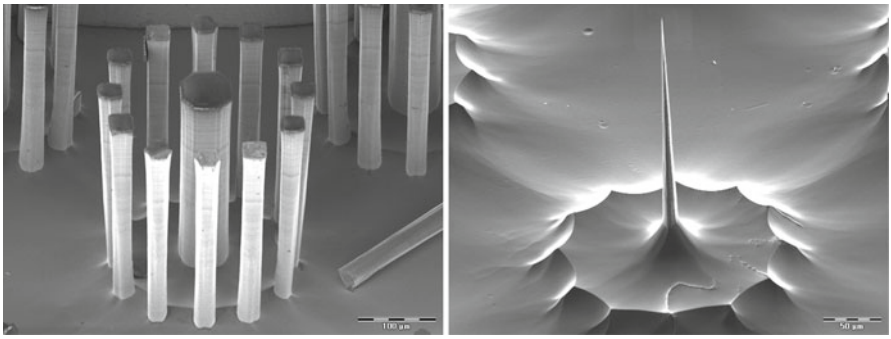

Fig. 5.28 Silicon probes fabricated with the utilization of ultrathin silicon wafers and performing double-side fabrication. Scale bar is 100 μm on the *left* and 50 μm on the *right*. Reproduced with permission from [70], © (2003) IOP Publishing. All rights reserved

One of the more interesting fabrication approaches to integrate on-chip silicon probes and silicon dioxide microtubes is reported from Toyohashi University of Technology (Toyohashi, Japan). The researchers at this university have successfully developed a process by which they *grow* silicon and oxide microtubes on-chip utilizing a vapor–liquid–solid (VLS) method [72–74]. Interconnection materials such as tungsten, tungsten silicide, titanium nitride, and titanium are used to ensure that the Si and SiO_2 probes make contact with the Metal Oxide Semiconductor Field Effect Transistors (MOSFETs) that are fabricated in the first step of the process (Fig. 5.29). The MOSFETs are fabricated utilizing a standard 5 μm CMOS process. For the formation of the silicon probes, a 160 nm gold film was selectively deposited as a catalyst. VLS growth was carried out in a gas source molecular beam epitaxy (MBE) system with Si_2H_6 gas while heating the substrate to 680 °C. An Au–Si alloy is formed first by heating the substrate before the VLS growth. Phosphorous thermal diffusion can be carried out to reduce the resistivity of the probes. In order to create the microtubes, a silicon dioxide layer was grown on the tubes utilizing PECVD. This oxide is patterned utilizing standard photolithography, followed by wet etching, and once the gold–silicon alloy is removed, a XeF_2 etch is utilized to remove the silicon in the tube to create silicon dioxide-coated microtubes. The probes and microtubes are shown in Fig. 5.30. The probes and tubes are typically ~3 μm in diameter and ~30 μm in height.

5.3 Metal, Glass, and Polymer Probes as 3-D MEAs

Even though silicon has been the major material for the fabrication of three-dimensional MEAs, researchers in the last 15 years have looked to other materials due to several reasons: (a) costs associated with clean room microfabrication; (b) many universities may not have access to a high-class clean room; (c) end users of this tool (neuroscientists, physicians, cardiologists, toxicologists, pharmacologists, etc.) are very familiar with materials like polymers and biocompatible metals.

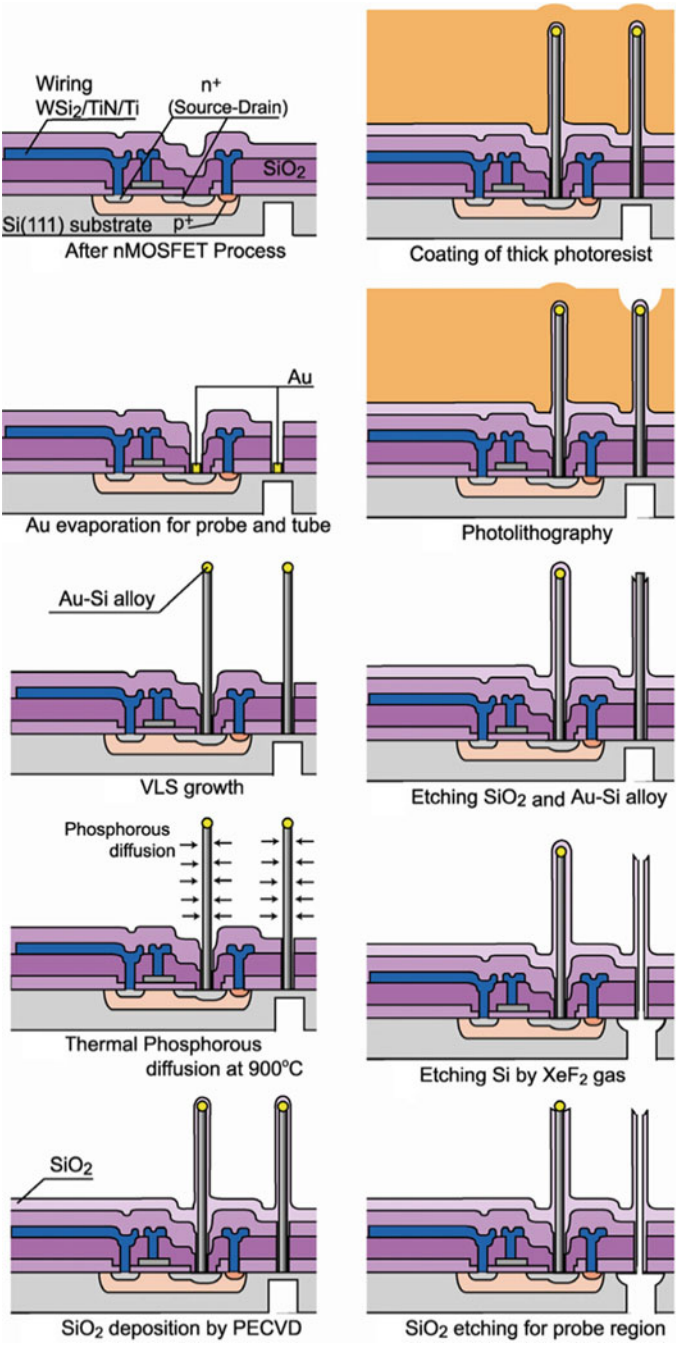

Fig. 5.29 Process flow for the fabrication of Si and SiO_2 probe arrays utilizing the VLS technique. Reproduced with permission from [74], © (2008) IOP Publishing. All rights reserved

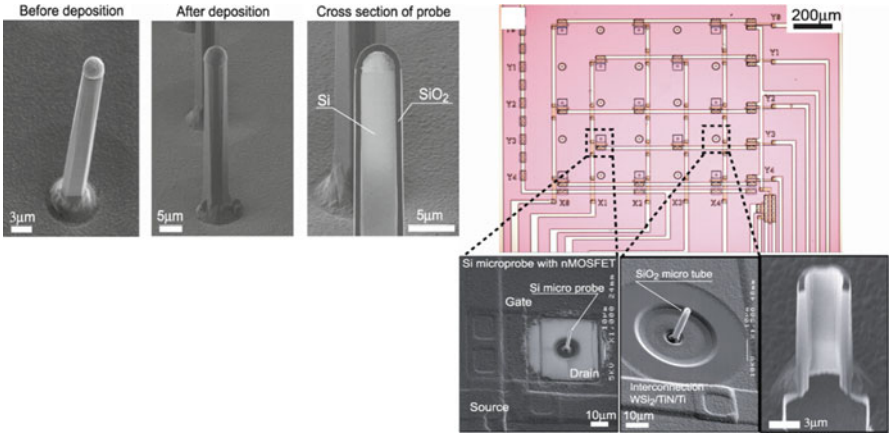

Fig. 5.30 Optical image of a MOSFET with regions of Si and SiO_2 nano-probe arrays (SEMs) on the *right*. SEM images of the microprobes on the *left*. Reproduced with permission from [74], © (2008) IOP Publishing. All rights reserved

Thus MEMS technologies developed on these materials are more likely to enjoy easy adoption and (d) many of the materials mentioned enjoy superior properties (such as mechanical stiffness comparable to tissue/cell networks and biocompatibility) to interface with cell cultures and tissue as compared to silicon.

Examples of such nonconventional approaches include glass micromachining, micromolding-based approaches, SU-8 micromachining, polyimide micromachining, electrical discharge micromachining, parylene-based approaches, etc. Some of these approaches are detailed below.

5.3.1 EDM-Based 3-D MEAs

Electrical discharge machining (EDM) is a process that makes use of computer-aided design (CAD) that runs under computer numerical control (CNC) and is capable of batch processing. It is used to generate intricate features with high aspect ratios and is capable of machining a large variety of conductive materials.

Fofonoff et al. [75–77] describe the use of EDM technology toward the microfabrication of 3-D MEAs. A zinc-coated brass wire and the work piece (made of suitable metals) form the basic materials in this process. An initial cut through one plane perpendicular to the EDM wire was first made followed by a cut in the orthogonal direction. This group from the Massachusetts Institute of Technology (Cambridge, MA, USA) along with collaborators at the University of Chicago (Chicago, IL, USA) and Brown University (Providence, RI, USA) report the fabrication of 3-D MEAs from a variety of conductive materials—titanium, titanium–aluminum–vanadium alloy, stainless steel, and tungsten carbide as shown in Fig. 5.31.

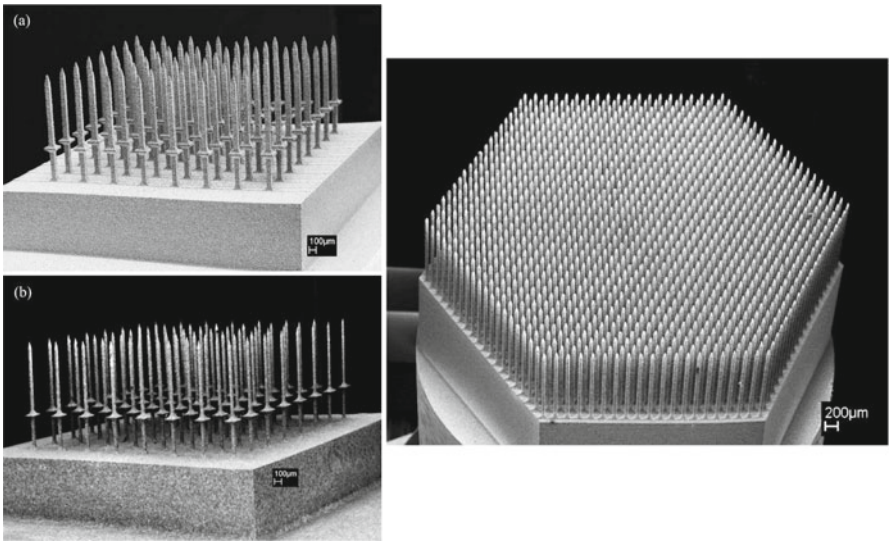

Fig. 5.31 SEM images electrical discharge machining (EDM)-based 3-D MEAs [77]

They report fabricating a variety of arrays with heights ranging from 1 to 5 mm and electrode widths ranging from 80 µm onward with interelectrode spacing ranging from 170 to 500 µm. They also report the fabrication of arrays with roughly 1,150 electrodes using this EDM technique. An etching step follows the EDM step where boiling hydrochloric acid (HCl) was utilized to not only prevent oxidation of the metals but also provide a suitable surface finish. The EDM wire 3-D MEA is subsequently electroplated with acid gold strike and platinum. The 3-D MEA was further insulated with parylene-C chosen due to its excellent biocompatibility [78] [Specialty Coating Systems Inc. 2013]. Parylene can additionally be deposited conformally at room temperature. The insulation was exposed at the tips of the microelectrodes utilizing laser micromachining. A Resonetics Excimer laser was utilized for this purpose. This laser micromachines polymers at 248 nm by chemical ablation (breaking of bonds).

5.3.2 Glass-Based 3-D MEAs

Metz et al. [79] and Heuschkel et al. [80] report what is probably one of the first approaches to batch fabricate integrated 3-D MEAs *on-chip* (3-D MEAs built monolithically on a substrate using surface/bulk micromachining processes) specifically targeted at in vitro neural applications. A simplified process flow for such a technique is depicted in Fig. 5.32, and it begins with the deposition of chromium on float glass substrates. The substrates are 700 µm thick, and the deposition is carried out utilizing a sputtering process at high temperatures (455 °C). The deposition is followed by the definition of the chromium layer (used as a mask for subsequent

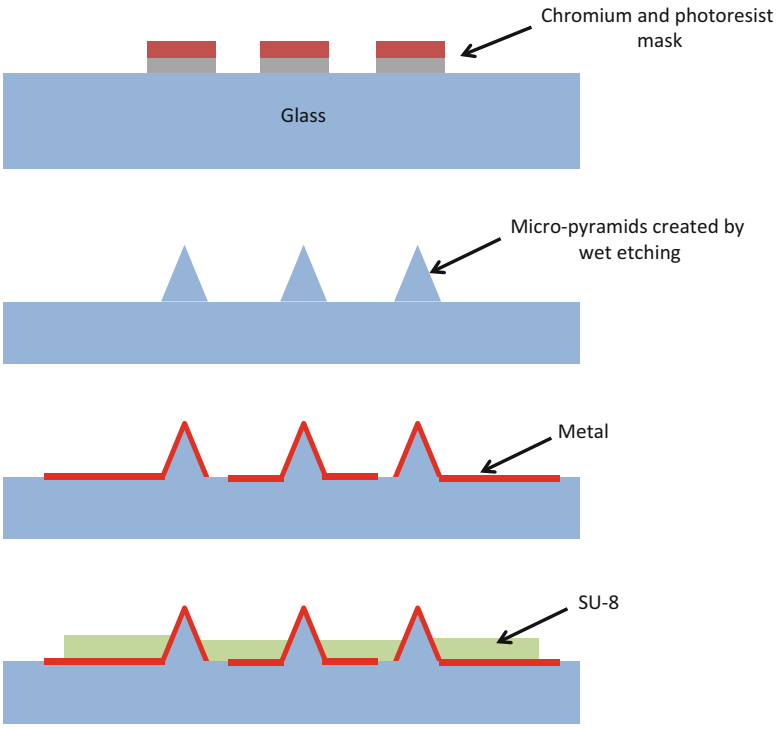

Fig. 5.32 Process flow for glass etching-/undercutting-based 3-D MEAs [79]

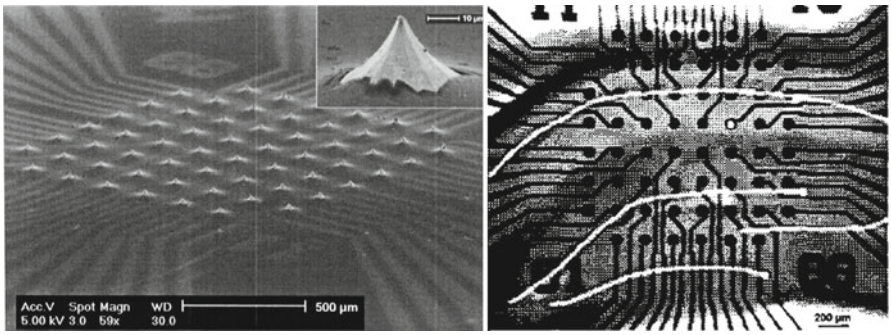

Fig. 5.33 SEM images of the microfabricated MEA (*left*) and a tissue slice placed on the MEA (*right*). Reproduced with permission from [80] © (2002) Elsevier

etching) using standard photolithography. The glass substrate was subsequently etched in a 10 % HF solution till the chromium mask was completely undercut and dethatched itself from the glass substrate. These researchers found out that chromium deposited at high temperatures was resistant enough to HF to carry out the etching. The HF etch step resulted in ~60 µm tall pyramidal structures that eventually will serve as the 3-D microelectrodes. Figure 5.33 depicts SEM images of such

electrodes and an optical image of a tissue slice on a 3-D MEA. In the next step, metal tracks were deposited and patterned to define a layer of titanium/platinum on the microelectrodes. The final step was the deposition and patterning of a 5 μm layer of SU-8 which serves as the insulation layer for the 3-D MEA. These 3-D MEAs are developed in an 8×8 matrix and are typically 40×40 μm^2 in area and have a pitch of 200 μm.

5.3.3 Polyimide- or Kapton-Based 3-D MEAs

Polyimide or Kapton is a popular material to construct 3-D MEAs, and these MEAs are typically designed to be implantable. The properties of polyimide that make it attractive are (a) mechanical flexibility; (b) electrically insulating properties; (c) surface chemistry amenable to modification and preparation that allow a host of bioactive organic species to be absorbed or covalently bonded to the surface of the material; (d) acceptable low gas permeability; (e) acceptable vapor transmission rates; and (f) biocompatibility [81].

Rousche et al. [82] demonstrate one such polyimide probe where the probe fabrication involves surface micromachining of photosensitive polyimide and chromium/gold metal layers. The metal layers are sandwiched between two layers of polyimide. Both layers are in between 10 and 20 μm thick, which makes these probes suitable for flexible applications. A RIE step with O_2 plasma is performed before the deposition of metal and the spin coating of the insulation layer of polyimide. This step serves to roughen the underlying layer for successful adhesion of the layer deposited on top. Several 2-D and 3-D probes have been fabricated with electrode sizes ranging from 20–40 μm×20–40 μm with shaft lengths up to 1.5 mm. Silicon is used as the carrier substrate, and the first step is the growth of a thermal layer of SiO_2 (0.5 μm thick). This layer serves as the release layer after probe fabrication.

Owens et al. [83], Boppart et al. [84], and Stieglitz et al. [85] also report similar fabrication processes for the fabrication of implantable 3-D MEAs constructed out of polyimide. Figure 5.34 depicts probes fabricated using this approach.

Tekuchi et al. from the University of Tokyo [86] report a similar approach where the third dimension for the probe is attained by bending the in-plane metal out of plane using a manual motion. Even though the mechanical match to tissue is vastly improved as compared to silicon or glass due to lower modulus of elasticity of polyimide, stiffness for insertion still remains an issue. A couple of researchers have investigated the strengthening of these probes using either a 5–10 μm thick silicon backbone or a molybdenum backbone [87, 88].

5.3.4 Parylene-Based 3-D MEAs Probes

Parylene belongs to the thermoplastic polymer family and was developed by Union Carbide in 1965 and has found its way into several industries such as PCBs due to

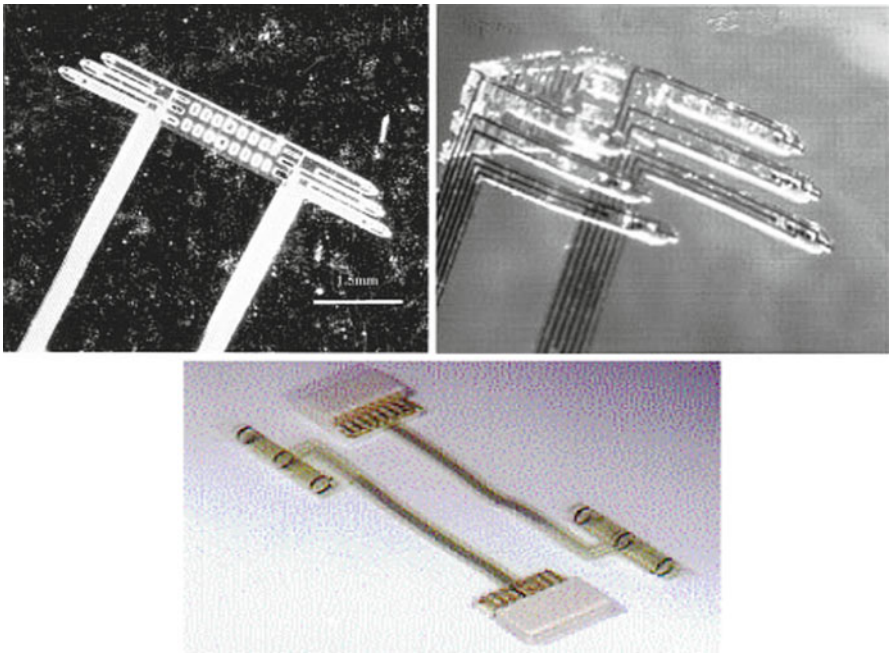

Fig. 5.34 Optical images of various approaches toward the microfabrication of polyimide-based 3-D MEA probes. *Top left* and *top right* [82]; *bottom*. Reproduced from [85], © (1999) The Author(s)

superior mechanical, chemical, biological, and thermal properties [78]. Additionally parylene can be deposited at room temperature making it ideal for low-temperature applications. Prof. Yu-Chong Tai's group at California Institute of Technology (Pasadena, CA, USA) has been leading the charge in the development of parylene-based 3-D MEAs.

Prof. Tai's group has been working in this area since 1999. Some of these efforts have been in the area of realization of neural cages [89, 90] that are fabricated with a multilayer parylene etching process utilizing multiple layers of photoresist as sacrificial layers. The neural cage acts as a "housing" structure for individual neurons with electrodes located right underneath the cage to stimulate and record from a neuron. Figure 5.35 depicts the SEM of one such cage.

Rodger et al. [91–93] report the development of a parylene MEMS technology for a retinal prosthetic system. High-density electrodes are fabricated on a parylene substrate with multiple layers of parylene deposition and etching with intermediate metallization processes. Additionally a parylene-based packaging technology has been developed to integrate the high-density array with an external CMOS chip for data processing [91, 94]. Figure 5.36 depicts a collage of parylene-based retinal MEAs and the packaging technologies associated with interfacing an ASIC with such a high-density probe.

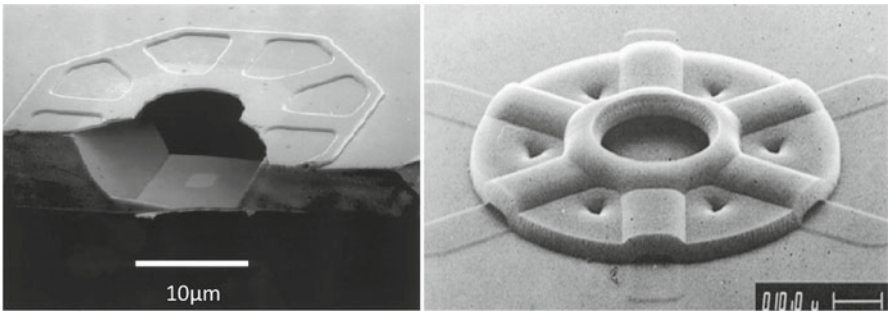

Fig. 5.35 SEM images of neural cages with microelectrodes located right below these cages fabricated by the MEMS group at the California Institute of Technology. *Left*, reproduced with permission from [89], © (1999) Elsevier; *right* [90]

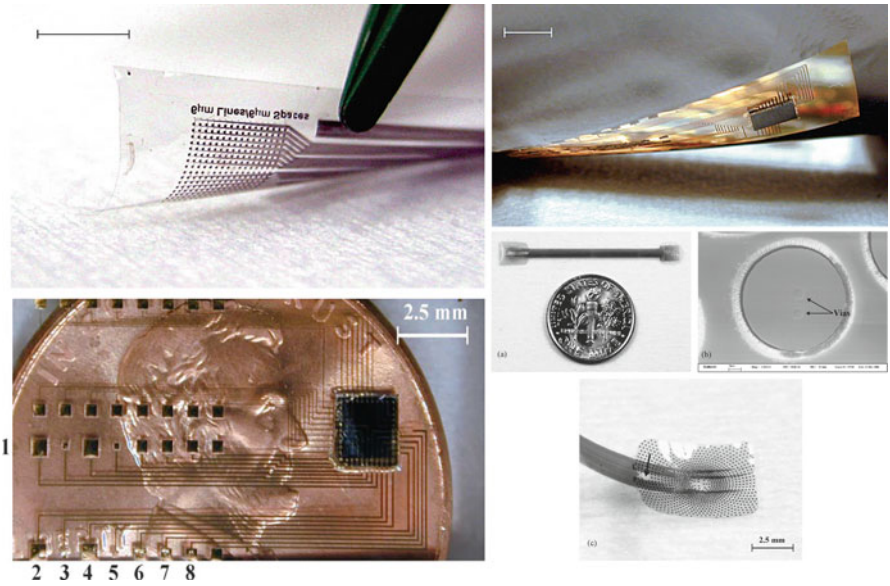

Fig. 5.36 Collage of parylene-based 3-D MEAs with and without a custom ASIC integrated for retinal prosthesis. *Top left*, *top right,* and *center left* [94]; *center right* and *bottom*, reproduced with permission from [83], © (2008) Elsevier

5.3.5 Three-Dimensional MEA Work at the Georgia Institute of Technology

Prof. Mark G. Allen's group at the Georgia Institute of Technology (Atlanta, GA, USA) has been working on the development of 3-D MEAs since the early 1990s. There are several reported technologies (all with metals or polymers or SU-8) developed both by Prof. Allen's group and Prof. Frazier's group from 1993 onward.

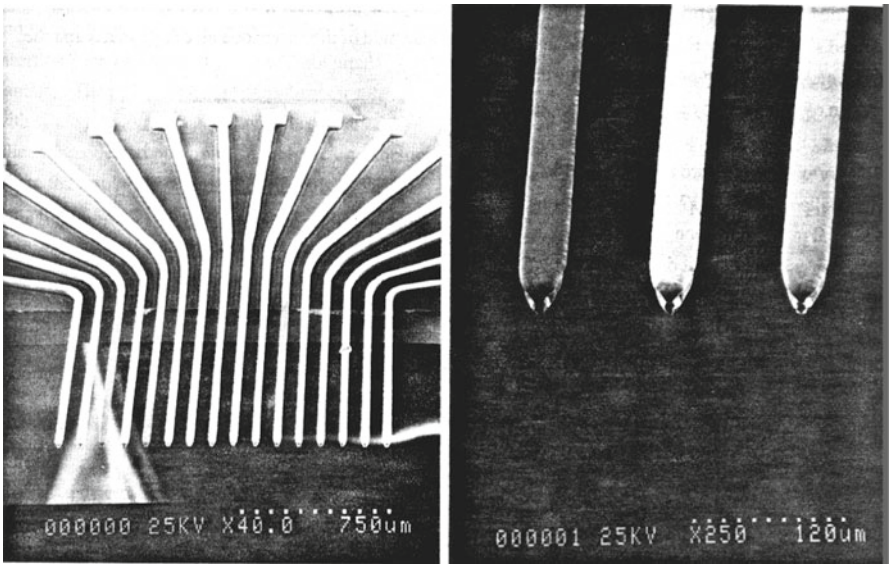

Fig. 5.37 One of the earliest demonstrations of metallic probes serving as 3-D MEAs fabricated on a silicon wafer using electrodeposition processes on a polyimide mold. The silicon wafer is etched in the final step to release the 3-D MEAs [95]

Frazier et al. [95, 96] report the fabrication of in-plane microelectrodes utilizing silicon as the substrate material onto which metallic probes are electroplated. The process begins with the doping of one side of the silicon wafer with boron to create a 4–6 μm thick p+ diffused layer. A 300 nm silicon nitride layer is then deposited on both sides of the wafer. The silicon nitride is patterned and etched on the undoped side to define the electrode area. This area is then etched anisotropically using a 20 % KOH solution, and the boron layer serves as an etch stop for the etching. The processing turns to the front side of the wafer now, and a seed layer of Ti/Cu is deposited on the silicon nitride layer. Polyimide is then spun coated and defined as an electroplating mold onto which several metallic probes can be electroformed. Gold, silver, nickel, copper, and combinations of these metals have been electroplated. The polyimide layer is then removed using a KOH solution, followed by the removal of the underlying seed layers used for electroplating. Silicon nitride insulation is then deposited and defined to open the recording sites. The probes are finally released by backside etching of the p+ membrane and the silicon nitride (Fig. 5.37). These probes are 15–20 μm in thickness, 25 μm in width, and roughly 1 mm long.

O'Brien et al. [97, 98] report a flexible microelectrode array (FMA) that can be sewn through a nerve for stimulation and recording from neural tissue applications. They utilize a glass substrate as the handle wafer on which the FMA is created. First a 10 μm × 10 mm long photolithographically defined gold metal traces are encapsulated within two layers of polyimide that are cured at 300 °C for 1 h to attain final mechanical strength. A sacrificial titanium mask is then defined. This Ti mask will be

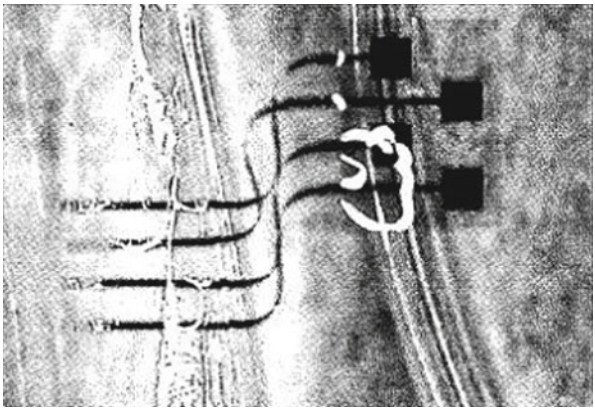

Fig. 5.38 Optical micrograph of a flexible microelectrode arrays (FMAs) fabricated on a polyimide substrate and inserted in a gelatin model [98]

used to define the FMA's outline, bond pads, and recording/stimulation sites. The rigid insertion piece of the device is then constructed by electroplating a metal layer using a thick photoresist mask. The photoresist layer is then removed followed by the removal of the metal seed layers. An RIE process is then utilized to define the recording sites and bond pads on the top polyimide layer. The FMA is released from the handle glass substrate by etching the Ti mask and immersing in DI water. Figure 5.38 depicts an optical micrograph of the released FMA inserted in a gelatin model.

Rowe et al. [99, 100] report an active 8×8 3-D microscaffold with integrated microelectrodes and microfluidic ports for culturing of neurons in vitro. The 3-D microscaffold consists of a silicon orifice plate above, which an 8×8 array of SU-8 micro-towers extends. The height of the micro-towers with integrated electrodes and fluidic channels extends to 1 or 1.5 mm from the silicon orifice plate as depicted in the schematic in Fig. 5.39. The SU-8 towers with the electrical and fluidic functionalities are fabricated in an *in-plane* fashion using a series of processes as described below. First a chromium release layer was deposited on a silicon wafer followed by the creation of the outer walls of the SU-8 towers utilizing a photolithographically defined layer of 5 μm SU-8. The outer wall layer houses the fluidic ports ($20 \times 20\ \mu m^2$) and electrodes ($15 \times 15\ \mu m^2$). Next 23 μm gold tabs were electrodeposited using a thick layer of AZ 4620 photoresist. The gold leads were then patterned and wet etched and subsequently insulated with a second 5 μm layer of SU-8. The hollow channel was defined in the next step utilizing a sacrificial layer of AZ 4620. A third SU-8 layer that is 75 μm thick was then defined to fabricate the outer wall of the SU-8 micro-tower. An intermediate layer of parylene-C is used to separate the SU-8 and the sacrificial resist layer. In the final release steps, the exposed parylene-C is etched using an RIE process, followed by the release of the towers by dissolving the sacrificial resist and lifting the towers off the substrate using chrome etch. The towers are then manually packaged into a DRIE-etched silicon orifice plate. Figure 5.40 depicts images of the microfabricated and assembled towers.

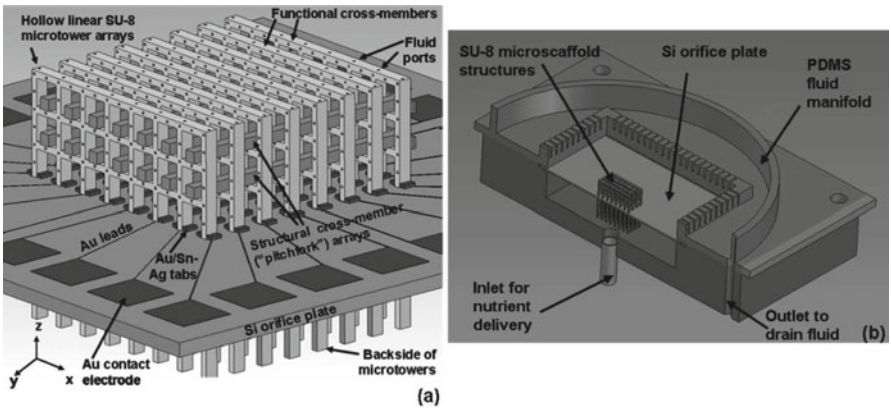

Fig. 5.39 Schematic of an 8×8 3-D SU-8 scaffold with integrated microelectrodes and microfluidic ports [100]

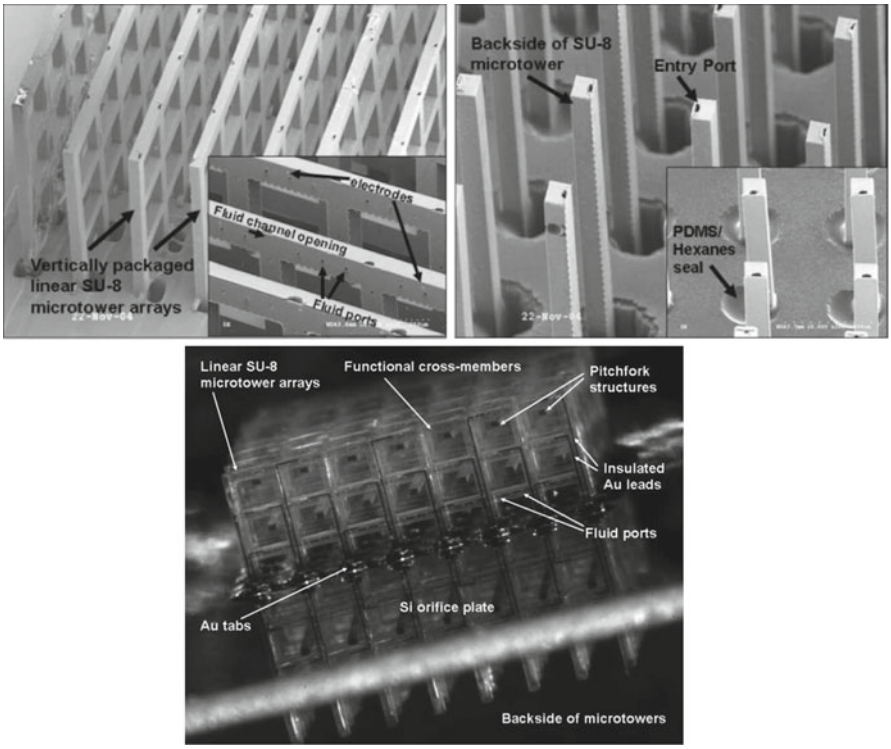

Fig. 5.40 SEM (*top*) and optical (*bottom*) images of the fabricated and assembled micro-towers with electrical and fluidic functionalities [100]

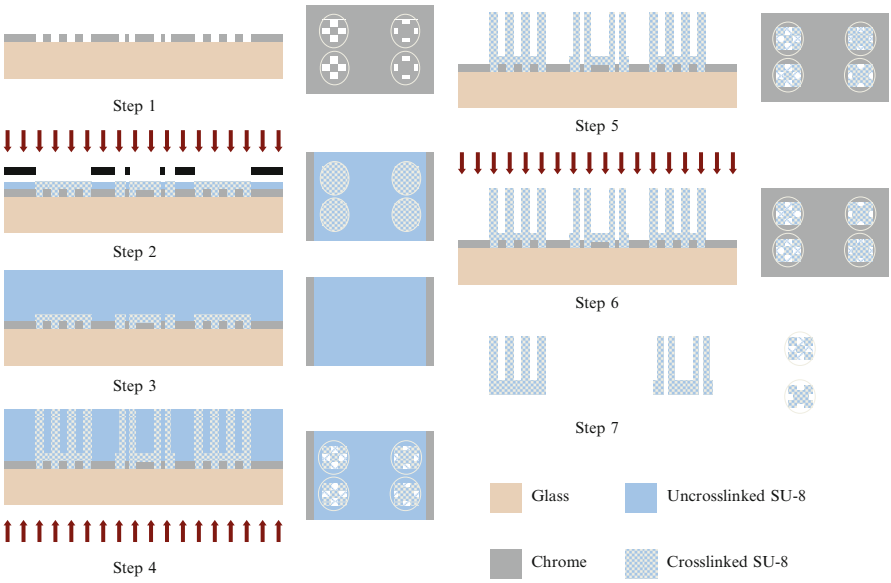

Fig. 5.41 Process flow for the fabrication of micro-towers utilizing a double-side exposure of SU-8 technology [101, 102]

Choi et al. [101] and Rajaraman et al. [102] report an SU-8-based active 3-D microscaffold technology with microelectrode and microfluidic functionalities. Their strategy is split into two different fabrication steps—(a) fabrication of micro-towers intended for electric or electric and fluidic functionalities and (b) addition of the 3-D microelectrode functionality in the second step. These 3-D coupled microfluidic, microelectrode MEAs have been utilized in a variety of in vitro network electrophysiological applications involving 2-D and 3-D cultures of neurons and tissue slices [103, 104].

Figures 5.41 and 5.42 depict the process flow for the fabrication of micro-towers. A novel "double-side" exposure technology of SU-8 is developed to fabricate the micro-towers in two steps. In the first step the base of the micro-towers is fabricated on a chrome plate (with features designed for bottom-side exposure) with a 100 µm thick layer of SU-8. A second layer of SU-8 (~500 µm thick) is then cast on the first layer without developing this layer. Bottom-side exposure of SU-8 is carried out with a larger UV energy dose. This exposure energy is coupled into SU-8 through the designed features in the chrome mask. Both layers are simultaneously developed thus defining ~500 µm tall SU-8 towers on a SU-8 substrate. These micro-towers are then individualized, and seed layers of Ti/Cu (30 nm/900 nm) are coated onto the towers. Parylene-C is then conformally coated onto the metallized micro-towers. This parylene layer is subsequently laser micromachined using a UV laser to define metal traces in 2-D and 3-D. Nickel is then electrodeposited onto the laser micromachined metal track areas to define the 2-D and 3-D microelectrodes.

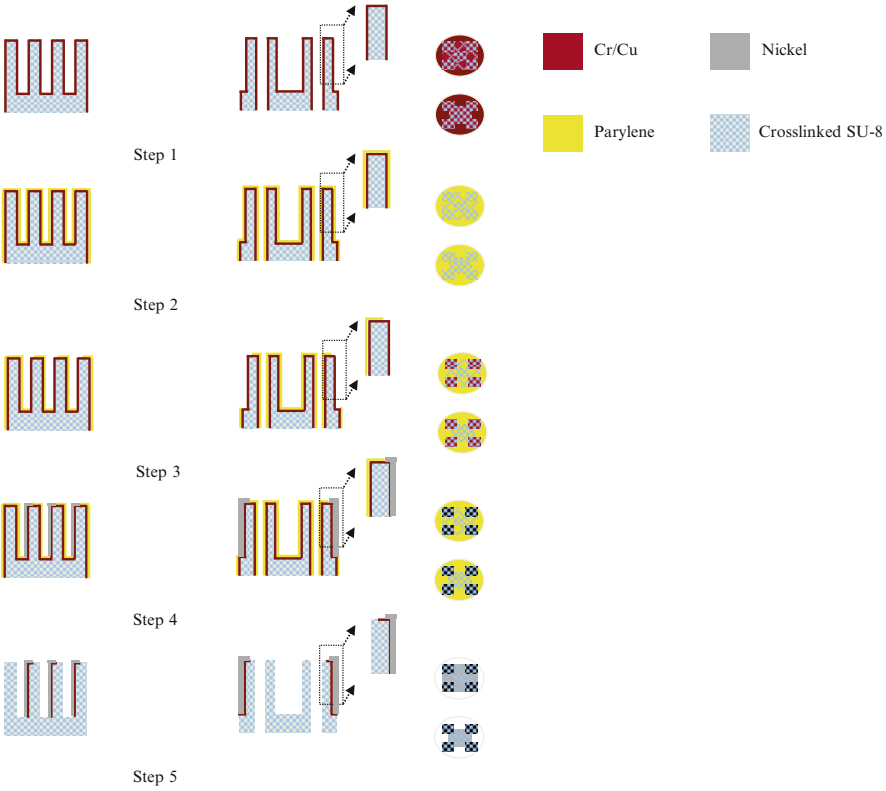

Fig. 5.42 Process flow for the fabrication of micro-towers utilizing a double-side exposure of SU-8 technology. These steps depict the fabrication of the microelectrodes on the micro-towers. [101, 102]

Figure 5.43 depicts images of the micro-towers and metal defined on the micro-towers. Thus, utilizing nonconventional microfabrication technologies such as "double-side" SU-8 exposure, laser micromachining, and electroplating, 3-D MEAs are created in a monolithic fashion with electrodes as tall as 500 μm and above. These devices are further packaged utilizing traditional approaches, and a thick insulation (parylene-C) is conformally deposited over 2-D and 3-D topographies to allow for cell cultures to seed onto a friendly material (parylene-C). Platinum is further electroplated in the last step to define the recording sites (process steps, images not shown).

Metal transfer micromolding (MTM) technology is an ideal technological platform for 3-D MEAs. It is a technology that has been pioneered by Prof. Allen's group [106] that has been used as a platform for the microfabrication of microneedles, RF MEMS components flow sensors, cellular scaffolds, and 3-D MEAs.

Rajaraman et al. [29, 105] report two different microfabrication approaches as shown in Figs. 5.44 and 5.45 for in vitro and in vivo 3-D MEAs respectively. The former starts with the exposure of pyramidal tips on 700 μm SU-8 utilizing inclined UV lithography. A silicon wafer is used as a carrier substrate on which the

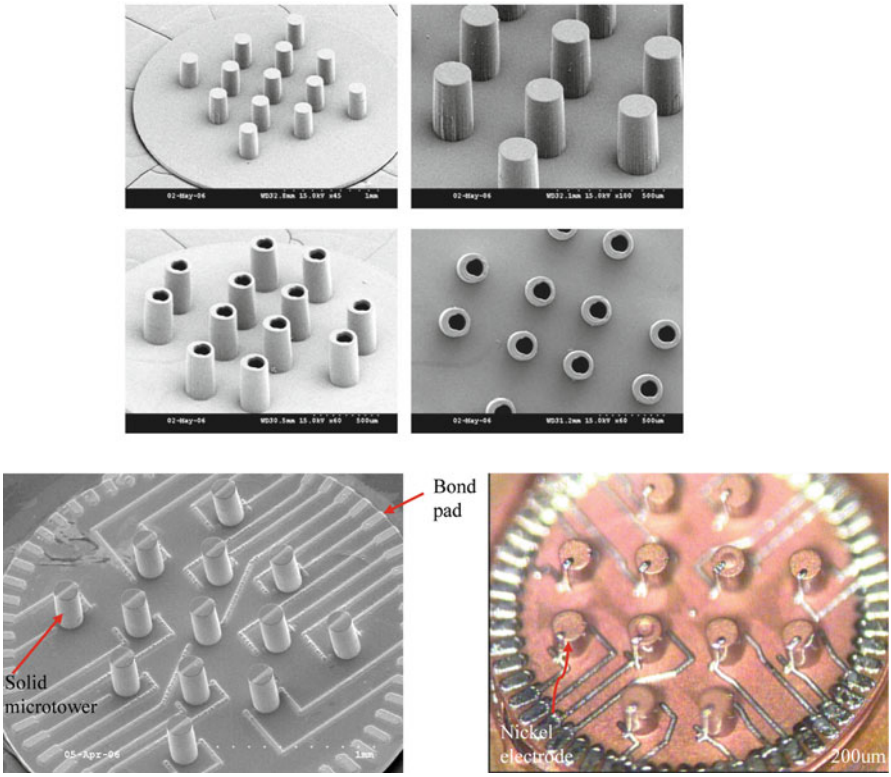

Fig. 5.43 SEM of the micro-towers fabricated utilizing double-side exposure technology (*top*). SEM and optical images of the 3-D microelectrodes defined on these towers (*bottom*). Reproduced with permission from [104], © (2007) IOP Publishing. All Rights Reserved

microfabrication is performed. A second layer of SU-8 (100 μm thick) is spin coated and exposed with the metal interconnect pattern without developing the first layer. Both layers are simultaneously developed after a postexposure bake in order to obtain a two-layer SU-8 rigid mold. PDMS micromolding is carried out twice to create a flexible mold with the same pattern as the rigid mold. A layer of Cr/Au is used as the intermediate release layer between the two materials. To define the microelectrodes, a Au/Cr layer is deposited on the PDMS mold using either an e-beam or filament evaporator. Metal transfer is achieved by bringing a high-surface energy plate in contact with the PDMS mold. Metal is patterned at this step to create 2-D and 3-D microelectrodes (up to a height of 500 μm is reported). Once the metal is patterned, the target polymer is cast into the patterned PDMS mold and processed. The final 3-D MEA structure is demolded in the last step with patterned microelectrodes. For the in vivo 3-D MEAs, the metal interconnect lithography step is eliminated, as each demolded array is a separate electrode in itself. Figure 5.46 depicts SEM and optical images of 3-D MEAs constructed with the metal transfer

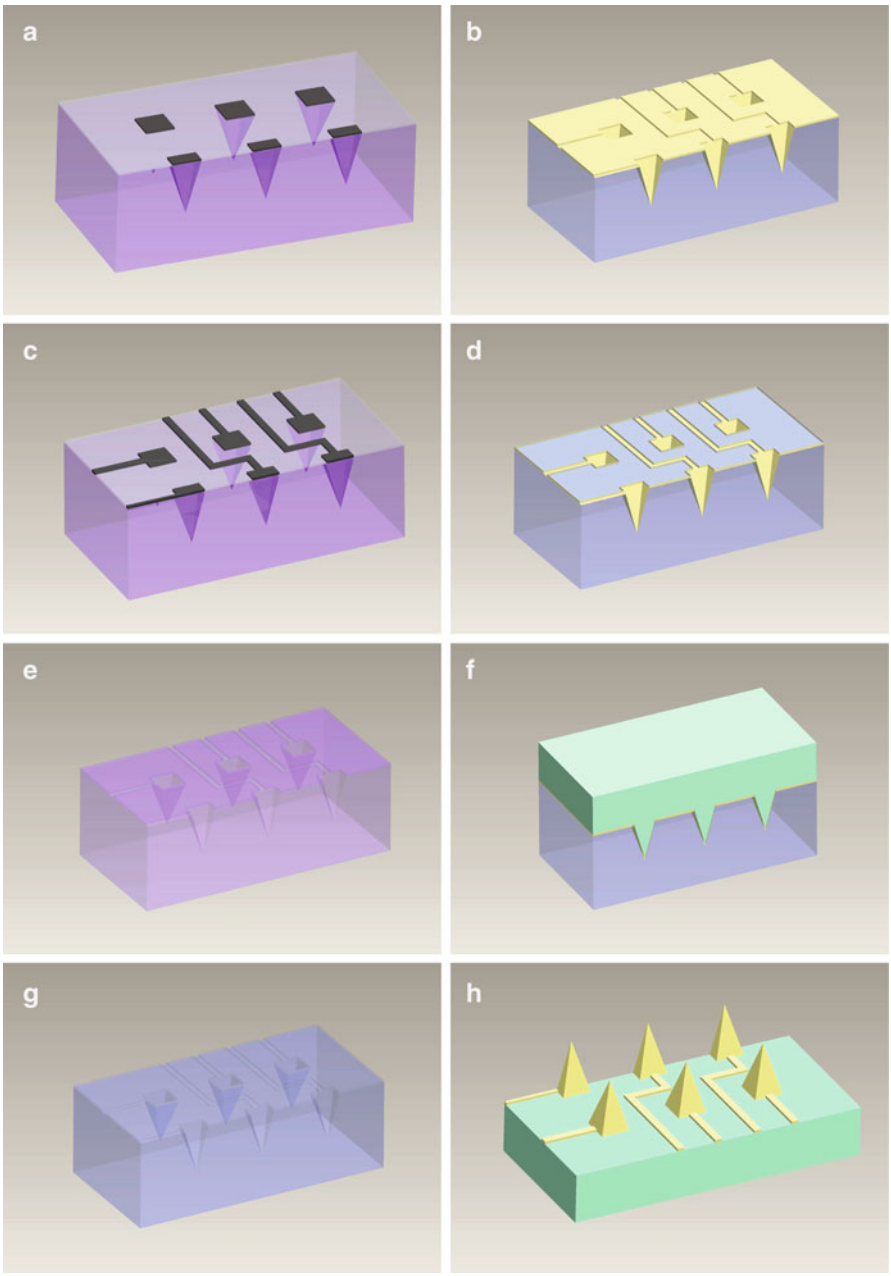

Fig. 5.44 Process flow for the fabrication of 3-D MEAs utilizing metal transfer micromolding technology [105]

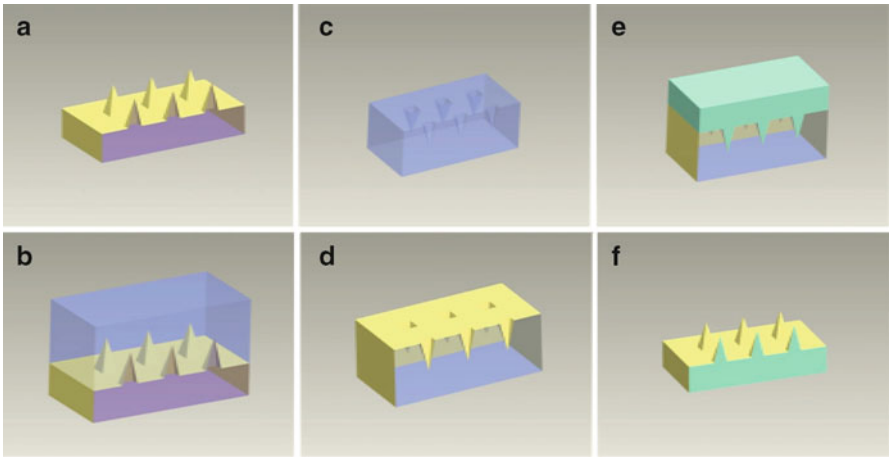

Fig. 5.45 Process flow for the fabrication of in vivo 3-D MEAs utilizing metal transfer micromolding technology. The master structure (**a**) can be fabricated using different techniques—inclined rotational exposure of SU-8 or double-side exposure of SU-8 followed by RIE sharpening. Reproduced with permission from [29], © (2011) IOP Publishing. All Rights Reserved

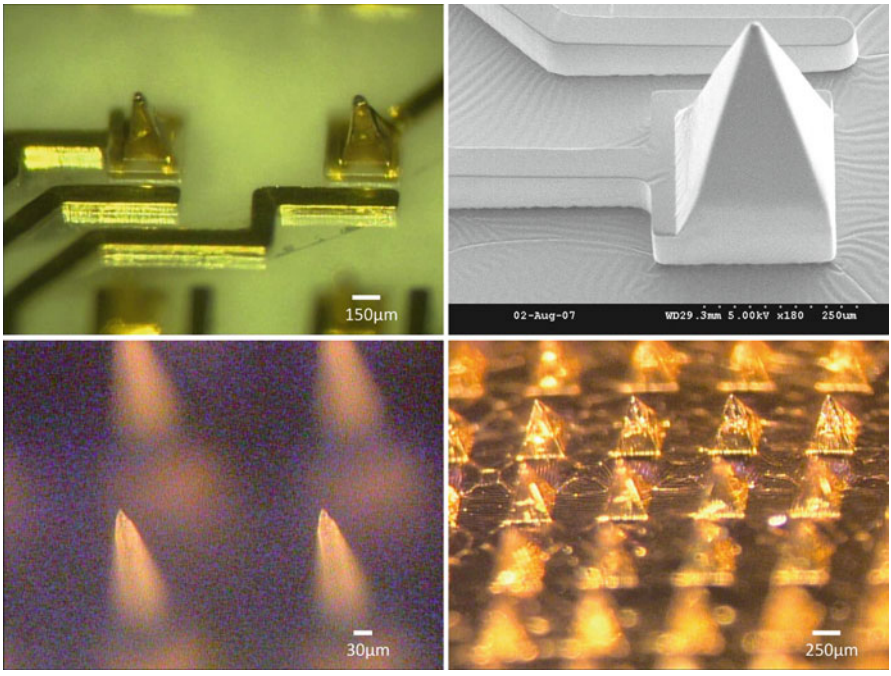

Fig. 5.46 SEM and optical micrographs of the 3-D MEAs fabricated utilizing the metal transfer micromolding technology for in vitro and in vivo applications. *Bottom left* and *bottom right*, reproduced with permission from [29], © (2011) IOP Publishing; (*top left* and *top right*) [105]

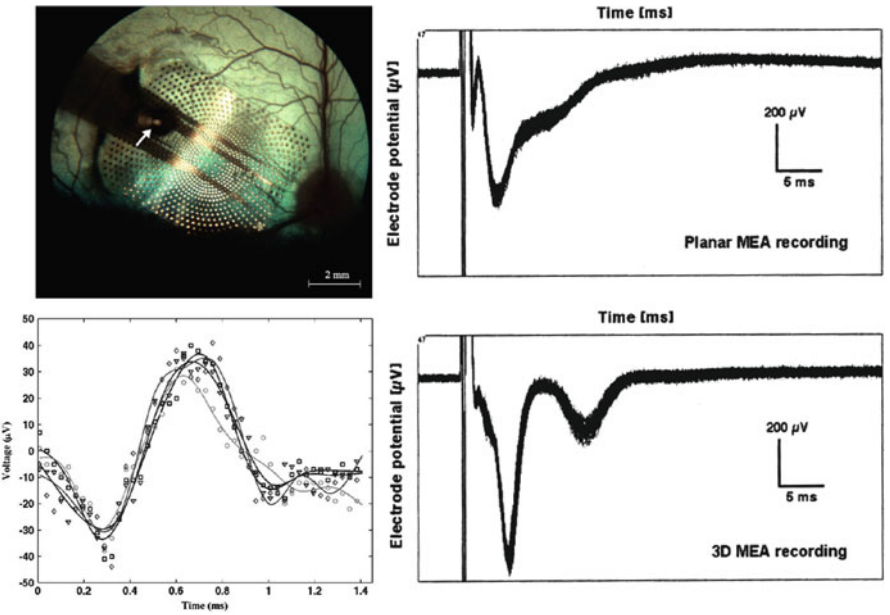

Fig. 5.47 Fundus photograph of a parylene 3-D MEAs tacked to a retina (*top left*, reproduced with permission from [92] © (2008) Elsevier); comparison between a single electrode in a planar and 3-D glass MEA showing much better spike signal acquisition in a rat hippocampal tissue slice (*top right*, reproduced with permission from [80] © (2002) Elsevier Heuschkel); spike recording from the cortex of a mouse using the EDM 3-D MEA (*bottom left* [77])

micromolding technology. For the in vitro 3-D MEAs, a parylene layer is conformally evaporated on a packaged device and patterned using laser micromachining to define the final electrode structure. The approach also reports the development of platinum electroplating on a packaged device to demonstrate low-impedance microelectrodes (results not shown).

Such metal-, polymer-, and SU-8-based technologies are becoming more popular with end users of these devices. Though not as thoroughly characterized as the silicon devices, several applications have been built on these devices. Examples of data acquisition from polymer-, glass-, SU-8-, and metal-based 3-D MEAs are depicted in Figs. 5.47 and 5.48. These images show the efficacy of these MEAs in biological experimentation.

5.4 Concluding Remarks

Microelectrode arrays (MEAs) are important tools for scientific discovery and medical advancement. Over the past 45 years, several three-dimensional MEA technologies have been developed and characterized worldwide. These technologies

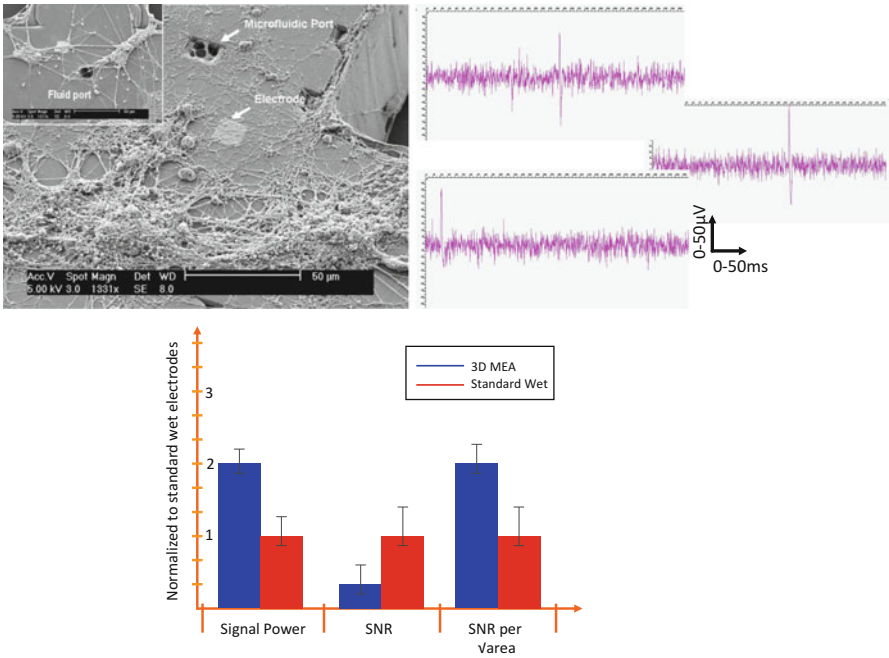

Fig. 5.48 Examples of applications developed on the Georgia Tech 3-D MEAs. An in vitro hippocampal neuronal culture on an SU-8 3-D MEA (*top left* [100]); action potential recordings from several electrodes utilizing MTM 3-D MEAs and tissue slice electrophysiology (*top right* [105]); and comparison of EMG data acquired on test human subjects between a MTM 3-D MEA and standard wet electrodes (*bottom*, reproduced with permission from [29], © (2011) IOP Publishing)

traditionally emanated from the IC fabrication industry, and hence many of the early processing techniques are based on using silicon as a substrate. To this day silicon-based 3-D MEAs remain the most well-characterized tools with extensive commercial and academic applications reported by several groups. As silicon technology continues to develop, so does the development of new and innovative fabrication methodologies for the construction of 3-D MEAs.

In the last 15 years, non-silicon-based approaches have gained a lot of traction. One of the big attractions toward moving away from silicon is familiarity of materials such as polymers for the end users of this technology. Several 3-D MEA microfabrication technologies have been reported on glass, metal, polyimide, parylene, SU-8, PDMS, and other polymer substrates. Though not as well characterized as silicon-based 3-D MEAs, the application development on these tools has increased in the last 5 years.

This chapter summarizes advances in both traditional silicon based and non-traditional Micro-Electro-Mechanical Systems (MEMS) approaches to the fabrication of 3-D MEAs. These MEAs will continue to serve as very important tools that have led to dramatic advances in the areas of neuroscience, prosthetics, pharmacology, diagnostics and implantable devices.

References

1. Galvani, L.: De Viribus Electricitatis in Motu Musculari Commentarius. In: De Bononiensi Scientiarum et Artium Instituto atque Academia Commentarii, vol. VII, Bononiae, Ex Typographia Instituti Scientiarum (1791)
2. Chowdhury, T.K.: Fabrication of extremely fine glass Micropipette Electrodes. Journal of Scientific Instruments **2**(12), 1087–1090 (1969)
3. Gray, C.M., Maldonado, P.E., Wilson, M. et al.: Tetrodes markedly improve the reliability and yield of multiple single-unit isolation from multi-unit recordings in cat striate cortex. J. Neurosc. Meth. **63**(1–2), 43–54 (1995)
4. Fishman, H.M.: Patch Voltage Clamp of a Squid Axon Membrane. Journal of Membrane Biology **24**(3–4), 265–279 (1975)
5. Chiappalone, M., Casagrande, S., Tedesco, M., Valtorta, F., Baldelli, P., Martinoia, S., Benfenati, F.: Opposite Changes in Glutamatergic and GABAergic Transmission Underlie the Diffuse Hyperexcitability of Synapsin I-Deficient Cortical Networks. Cerebral Cortex **19**(6), 1422–1439 (2009)
6. Cao, Z., Hulsizer, S., Tassone, F., Tang, H.T., Hagerman, R.J., Rogawski, M.A., Hagerman, P.J., Pessah, I.N.: Clustered burst firing in FMR1 premutation hippocampal neurons: amelioration with allopregnanolone. Hum. Mol. Genet. **21**(13), 2923–2935 (2012)
7. MacLaren, E.J., Charlesworth, P., Coba M.P., Grant, S.G.: Knockdown of mental disorder susceptibility genes disrupts neuronal network physiology in vitro. Mol. Cell. Neurosci. **47**(2), 93–99 (2011)
8. Morin, F.O., Takamura, Y., Tamiya, E.: Investigating neuronal activity with planar microelectrode arrays: Achievements and new perspectives. Journal of Bioscience and Bioengineering **100**, 131–143 (2005)
9. McConnell, E.R., McClain, M.A., Ross, J., LeFew, W.R. and Shafer, T.J.: Evaluation of multi-well microelectrode arrays for neurotoxicity screening using a chemical training set. NeuroToxicology **33**(5), 1048–1057 (2012)
10. Lignani, G., Raimondi, A., Ferrea, E., Rocchi, A., Paonessa, F., Cesca, F., Orlando, M., Tkatch, T., Valtorta F., Cossette, P., Baldelli, P., and Benfanati, F.: Epileptogenic Q555X SYN1 Mutant Triggers Imbalances in Release Dynamics and Short-Term Plasticity. Hum. Mol. Genet. **22**, (11), 2186–9219 (2013)
11. Wong, R.O.L., Meister, M., Shatz, C.J.: Transient Period of Correlated Bursting Activity During Development of the Mammalian Retina. Neuron **11**, 923–938 (1993)
12. Wagenaar, D.A., Madhavan, R., Pine, J., Potter, S.M.: Controlling bursting in cortical cultures with closed-loop multi-electrode stimulation. Journal of Neuroscience **25**, 680–688 (2005)
13. Haustein, M.D., Reinert, T., Warnatsch, A.: Synaptic transmission and short-term plasticity at the calyx of Held synapse revealed by multielectrode array recordings. Journal of Neuroscience Methods **174**(2), 227–236 (2008)
14. Bastrikova N., Gardner, G.A., Reece, J.M.: Synapse elimination accompanies functional plasticity in hippocampal neurons. Proceedings of the National Academy of Sciences **105**(8), 3123–3127 (2008)
15. Jimbo, Y., Tateno, T., Robinson, H.P.C.: Simultaneous induction of pathway-specific potentiation and depression in networks of cortical neurons. Biophysical Journal **76**, 670–678 (1999)
16. Dunlap, J., Bowlby, M., Peri, R.: High-throughput electrophysiology: an emerging paradigm for ion-channel screening and physiology. Nature Reviews Drug Discovery **7**(4), 358–368 (2008)
17. Chiappalone, M., Vato, A., Tedesco, M.B., Marcoli, M., Davide, F., Martinoia, S.: Networks of neurons coupled to microelectrode arrays: a neuronal sensory system for pharmacological applications. Biosensors & Bioelectronics **18**, 627–634 (2003)
18. Easter, A., Bell, M.E., Damewood, J.R., Redfern, W.S., Valentin, J-P., Winter, M.J., Fonck, C., Bialecki, R.A.: Approaches to Seizure Risk Assessment in Preclinical Drug Discovery. Drug Discovery Today **14**(17–18), 876–884 (2009)

19. Stett, A., Egert, U., Guenther, E., Hofmann, F., Meyer, T., Nisch, W., Haemmerle, H.: Biological application of microelectrode arrays in drug discovery and basic research. Analytical and Bioanalytical Chemistry **377**, 486–495 (2003)
20. Meyer, D.A., Carter, J.M., Johnstone, A.F., Shafer, T.J.: Pyrethroid Modulation of Spontaneous Neuronal Excitability and Neurotransmission in Hippocampal Neurons in Culture. Neurotoxicology **29**(2): 213–225 (2008)
21. Martinoia, S., Bonzano, L., Chiappalone, A.: In vitro cortical neuronal networks as a new high-sensitive system for biosensing applications. Biosensors and Bioelectronics **20**(10), 2071–2078 (2005)
22. Gholmieh, G., Courellis, S., Fakheri, S., Cheung, E., Marmarelis, V., Baudry, M., Berger, T.: Detection and classification of neurotoxins using a novel short-term plasticity quantification method. Biosensors & Bioelectronics **18**, 1467–1478 (2003)
23. Kovacs, G.T.A.: Electronic sensors with living cellular components. Proceedings of the IEEE **91**(6), 915–929 (2003)
24. DeBusschere, B.D., and Kovacs, G.T.A.: Portable cell-based biosensor system using integrated CMOS cell-cartridges. Biosensors and Bioelectronics **16**, 543–556 (2001)
25. Wise, K.D.: Silicon microsystems for neuroscience and neural prostheses. Engineering in Medicine and Biology Magazine, IEEE **24**(5), 22–29 (2005)
26. Normann, R.A.: Technology Insight: future neuroprosthetic therapies for disorders of the nervous system. Nature Clinical Practice Neurology **3**(8), 444–452 (2007)
27. Griss, P., Enoksson, P., Tolvanen-Laakso, H.K., Merilainen, P., Ollmar, S., and Stemme, G.: Micromachined Electrodes for Biopotential Measurements. IEEE Journal of Microelectromechanical Systems **10**(1), 10–16 (2001)
28. Ruther, P., Lapatki, B., Trautmann, A., and Paul, O.: Micro Needle Based Electrode Arrays for Surface Electromyography. Mikrosystemtechnik Kongress, October, Dresden, Germany. VDE Verlag, Berlin, Offenbach, Germany (2007)
29. Rajaraman, S., Bragg, J.A., Ross, J.D., and Allen, M.G.: Micromachined Three-Dimensional Electrode Arrays for Transcutaneous Nerve Tracking. Journal of Micromechanics and Microengineering **21**(8), 085014 (2011)
30. Plummer, J.D., and Meindl, J.D.: Micropower Electronics for a Reading Aid for the Blind. IEEE J. Solid State Circuits **7**(2), 111–119 (1972)
31. Allen, H.V., Knutti, J.W., and Meindl, J.D.: Integrated circuits for an Implantable Pulsed Doppler Ultrasonic Blood Flowmeter. IEEE J. Solid State Circuits **13**(6), 853–863 (1978)
32. Samaun, Wise, K.D., and Angell, J.B.: An IC Piezoresistive Pressure Sensor for Biomedical Instrumentation. IEEE Trans. Biomed. Engr. **20**(3), 101–109 (1973)
33. Wise, K.D., Angell, J.B., and Starr, A.: An Integrated Circuit Approach to Extracellular Microelectrodes. Proc. of Intrl Conf. on Med and Bio Engr., 14–15 (1969)
34. Wise K.D., and Angell, J.B.: A Low-Capacitance Multielectrode Probe for Use in Extracellular Neurophysiology. Biomedical Engineering, IEEE Transactions on **BME-22**(3), 212–219 (1975)
35. Najafi, K., Wise, K.D., and Mochizuki, T.: A High Yield IC-Compatible Multichannel Recording Array. IEEE Transactions on Electron Devices **32**(7), 1206–1211 (1985)
36. Hoogerwerf, A.C., and Wise, K.D.: A Three-Dimensional Microelectrode Array for Chronic Neural Recording. IEEE Trans. Biomed. Engr. **41**(12), 1136–1146 (1994)
37. Wise, K.D., Anderson, D.J., Hetke, J.F., Kipke, D.R., and Najafi, K.: Wireless implantable microsystems: high-density electronic interfaces to the nervous system. Proceedings of the IEEE **92**(1), 76–97 (2004)
38. Bell T.E., Wise, K.D., and Anderson, D.J.: A flexible micromachined electrode array for a cochlear prosthesis. Solid State Sensors and Actuators, 1997. TRANSDUCERS '97 Chicago., 1997 International Conference on **2**, 1315–1318 (1997)
39. Bell T.E., and Wise, K.D.: A dissolved wafer process using a porous silicon sacrificial layer and a lightly-doped bulk silicon etch-stop. Paper presented at the Eleventh Annual International Workshop on Micro Electro Mechanical Systems. MEMS 98. pp. 251–256, 25–29 January 1998

40. Huang, C., and Najafi, K.: Fabrication of Ultrathin p++ Silicon Microstructures using Ion Implantation and Boron Etch Stop. IEEE Journal of MicroElectroMechanical Systems (JMEMS) **10**, 532–537 (2001)
41. Ghovanloo, M., Beach, K., Wise, K.D., and Najafi, K.: A BiCMOS Wireless Interface Chip for Micromachined Stimulating Microprobes. IEEE EMBS Conference on Microtechnologies in Medicine and Biology, pp. 277–282, 2–4 May 2002
42. Bai Q., Wise, K.D., and Anderson, D.J.: A high-yield microassembly structure for three-dimensional microelectrode arrays. Biomedical Engineering, IEEE Transactions on **47**(3), 281–289 (2000)
43. Ghovanloo, M., and Najafi, K.: A Three-Dimensional Microassembly Structure for Micromachined Planar Microelectrode Arrays. Proc. IEEE EMBS Conf., pp. 112–115 (2005)
44. Merriam, M.E., Srivannavit, O., Gulari, M.N., Wise, K.D.: A Three-Dimensional 64-Site Folded Electrode Array using Planar Fabrication. IEEE Journal of Microelectromechanical Systems. **20**(3), 594–600 (2011)
45. Papageorgiou, D.P., Shore, S.E., Bledsoe, S.C., Wise, K.D.: A Shuttered Neural Probe with On-Chip Flowmeters for Chronic in-vivo Drug Delivery. IEEE Journal of Microelectromechanical Systems **15**(4), 1025–1033 (2006)
46. NeuroNexus (2013) http://www.neuronexus.com
47. Campbell, P.K., Jones, K.E., Huber, R.J., Horch, K.W., and Normann, R.A.: A Silicon-based, 3-Dimensional Neural Interface - Manufacturing Processes for an Intracortical Electrode Array. IEEE Transactions on Biomedical Engineering **38**(8), 758–768 (1991)
48. Jones, K.E., Campbell, P.K., and Normann, R.A.: A Glass Silicon Composite Introcortical Electrode Array. Annals of Biomedical Engineering **20**(4), 423–437 (1992)
49. Sharma, A., Rieth, L., Tathireddy, P., Harrison, R., Oppermann, H., Klein, M., Topper, M., Jung, E., Normann, R., Clark, G., and Solzbacher, F.: Long-term in-vitro Functional Stability and Recording Longevity of Fully Integrated Wireless Neural Interfaces based on the Utah Slant Electrode Array. Journal of Neural Engineering **8**, 045005 (2011.)
50. Rousche, P.J., Normann, R.A.: Chronic Recording Capability of the Utah Intracortical Electrode Array in a cat sensory cortex. Journal of Neuroscience Methods **82**, 1–15 (1998)
51. Bhandari, R., Negi, S., Rieth, L., Normann, R.A., and Solzbacher, F.: A novel masking method for high aspect ratio penetrating microelectrode arrays. J. Micromech. Microeng. **19**, 035004 (8pp) (2009)
52. Nordhausen, C.T., Maynard, E.M., and Normann, R.A.: Single unit Recording Capabilities of a 100 Microelectrode Array. Brain Research **726**, 129–140 (1996)
53. Blackrock Microsystems Inc. (2013) http://www.blackrockmicro.com
54. Brenner, A., Stein R.B., and Normann, R.A.: Selective Stimulation of Cat Sciatic Nerve using an Array of Varying Length Microelectrodes. Journal of Neurophysiology **85**, 1585–1594 (2001)
55. Neves, H.P., and Ruther, P.: The NeuroProbes Project. NeuroProbes Consortium Report, (2007)
56. Stieglitz, T., Rubehn, B., Henle, C., Kisban, S., Hervik, S., Ruther, P., and Schuettler M.: Brain-Computer Interfaces: an Overview of the Hardware to Record Neural Signals from the Cortex. Prog. In Brain Research **175**(20), 297–315 (2009)
57. Kisban, S., Herwik, S., Seidl, K., Rubehn, B., Jezzini, A., Umiltà, M.A., Fogassi, L., Stieglitz, T., Paul, O., and Ruther, P.: Microprobe Array with Low Impedance Electrodes and Highly Flexible Polyimide Cables for Acute Neural Recording. IEEE EMBS, pp. 175–178, Lyon, 22–26 August 2007
58. Herwik, S., Kisban, S., Aarts A.A.A., Seidl, K., Girardeau, G., Benchenane, K., Zugaro, M.B., Wiener, S.I., Paul, O., Neves, H.P., and Ruther, P.: Fabrication Technology for Silicon-based Microprobe Arrays used in Acute and Sub-Chronic Neural Recording. Journal of Micromechanics and Microengineering **19**, 074008 (2009)
59. Neves, H., and Ruther, P.: NeuroProbes - Development of Multifunctional Probe Arrays for Cerebral Applications. R&D Fact Sheet (2008)
60. Aarts, A.A.A., Neves, H.P., Ulbert, I., Wittner, L., Grand, L., Fontes, M.B.A., Herwik, S., Kisban S., Paul, O., Puers, R.P., Ruther, P., and Van Hoof, C.: A 3D Silm-base Probe Array for In Vivo Recorded Neuron Activity. Proc. IEEE EMBS Conf., pp. 5798–5801 (2008)

61. Aarts A.A.A.: 3D Interconnect Technology for out-of-plane Biomedical probe arrays - a modular approach with slim-base solutions. Dissertation, Katholieke Universiteit Leuven (2011)
62. Spieth, S., Schumacher, A., Seidl, K., Hiltmann, K., Haeberle, S., McNamara, R., Dalley, J.W., Edgley, S.A., Ruther, P., and Zengerle, R.: Robust Microprobe Systems for Simultaneous Neural Recordings and Drug Delivery. Proc. IFMBE, pp. 2426–2430 (2008)
63. Spieth, S., Brett, O., Seidl, K., Aarts, AAA, Erismis, M.A., Herwik, S., Trenkle, F., Tatzner, S., Auber, J., Daub, M., Neves, H.P., Puers, R., Paul, O., Ruther, P., and Zengerle, R.: A Floating 3D Silicon Microprobe Array for Neural Drug Delivery Compatible with Electrical Recording. Journal of Micromechanics and Microengineering **21**, 125001 (16pp) (2011)
64. Aarts, A.A.A., Neves, H.P., Puers, R.P., Herwik, S., Seidl, K., Ruther, P., and Van Hoof, C.: A Slim out-of-plane 3D Implantable CMOS based Probe Array. Proc. Smart Systems Integration, pp. 258–263 (2009)
65. Seidl, K., Herwik, S., Nurcahyo, Y., Torfs, T., Keller, M., Schuttler, M., Neves, H., Stieglitz, T., Paul, O. and Ruther, P.: CMOS-Based High Density Silicon Microprobe Array for Electronic Depth Control in Neural Recording. Proc. IEEE (2009)
66. Frey, O., van der Wal, P.D., Spieth, S., Brett, O., Seidl, K., Paul, O., Ruther, P., Zengerle, R., and de Rooij, N.F.: Biosensor Microprobes with Integrated Microfluidic Channels for bi-directional Neurochemical Interaction. Journal of Neural Engineering, **8**, 066001 (2011)
67. Koo, K., Chung, H., Yu, Y., Seo, J., Park, J., Lim, J-M., Paik, S-J., Park, S., Choi, H.M., Jeong M-J., Kim, G.S., and Cho, D-I.: Fabrication of Pyramid Shaped Three-Dimensional 8x8 Electrodes for Artificial Retina. Sensors and Actuators A **130–131**, 609–615 (2006)
68. Kusko, M., Craciunoiu, F., Amuzescu, B., Halitzchi, F., Selescu, T., Radoi, A., Popescu, M., Simion, M., Bragaru, A., and Ignat, T.: Design, Fabrication and Characterization of a Low-Impedance 3-D Electrode Array System for Neuro-Electrophysiology. Sensors Journal **12**, 16571–16590 (2012)
69. Du, J., Roukes, M.L., and Masmanidis, S.C.: Dual-side and Three-Dimensional Microelectrode Arrays Fabricated from ultra-thin Silicon Substrates. Journal of Micromechanics and Microengineering **19**, 075008 (2009)
70. Hanein, Y., Schabmueller, C.G.J., Holman, G., Lucke, P., Denton, D.D., and Bohringer, K.F.: High Aspect Ration Submicrometer Needles for Intracellular Applications. Journal of Micromechanics and Microengineering **13**, S91–95 (2003)
71. Chu, H-Y., Kuo, T-Y. Chang, B., Chiao, C-C., and Fang, W.: Development of the Three-Dimensional Multi-Electrode Array for Neural Recording. Proc. IEEE Transducers Conf., pp. 1804–1807 (2005)
72. Harimoto, T., Takei, K., Kawano, T., Ishihara A., Kawashima, T., Kaneko H., Ishida, M., and Usui, S.: Enlarged Gold-Tipped Silicon Microprobe Arrays and Signal Compensation for Multi-site Electroretinogram Recordings in the Isolated Carp Retina. Biosensors and Bioelectronics **26**, 2368–7523 (2011)
73. Takei K., Kawashima, T., Takao, H., Sawada, K., and Ishida, M.: Si Micro Probe and SiO2 Micro Tube Array with NMOSFETs. Transducers 2007: The 14th International Conference on Solid-State Sensors, Actuators and Microsystems IEEE, pp. 1381–1384 (2007)
74. Takei, K., Kawashima, T., Kawano, T., Takao, H., Sawada, K., and Ishida, M.: Integration of out-of-plane Silicon Dioxide Microtubes, Silicon Microprobes and on-chip NMOSFETs by Selective Vapor-Liquid-Solid Growth. Journal of Micromechanics and Microengineering **18**, 035033 (2008)
75. Fofonoff, T.A., Martel, S., Wiseman, C., Dyer, R., Hunter, I.W., Hatsopoulos, N.G., and Donoghue, J.P.: A highly flexible manufacturing technique for microelectrode array fabrication. Engineering in Medicine and Biology, 2002. 24th Annual Conference and the Annual Fall Meeting of the Biomedical Engineering Society EMBS/BMES Conference, 2002. Proceedings of the Second Joint **3**, 2107–2108, Houston, Tx, USA, 23–26 October 2002
76. Fofonoff, T.A., Wiseman, C., Dyer, R., Malasek, J., Burgert, J., Martel, S., Hunter, I.W., Hatsopoulos, N.G., and Donoghue, J.P.: Mechanical assembly of a microelectrode array for use in a wireless intracortical recording device. 2nd Annual International IEEE EMBS

Special Topic Conf. on Microtechnologies in Medicine and Biology, pp. 269–72, Madison, Wisconsin USA, 24 May 2002
77. Fofonoff, T.A., Martel, S.M., Hatsopoulos, N.G., Donoghue, J.P., and Hunter, I.W.: Microelectrode array fabrication by electrical discharge machining and chemical etching. IEEE Transactions on Biomedical Engineering **51**(6), 890–895 (2004)
78. Specialty Coating Systems Inc. (2013) http://scscoatings.com
79. Metz, S., Heuschkel, M.O., Valencia Avila, B., Holzer, R., Bertrand, D., and Renaud, P.: Microelectrodes with Three-Dimensional Structures for Improved Neural Interfacing. Proc. of 23rd Annual EMBS Intr. Conf., IEEE, 765–768 (2001)
80. Heuschkel, M.O., Fejtl, M., Raggenbass, M., Bertrand, D., and Renaud, P.: A three-dimensional multi-electrode array for multi-site stimulation and recording in acute brain slices. Journal of Neuroscience Methods **114**(2), 135–148 (2002)
81. DuPont Inc. (2013) http://www2.dupont.com/Kapton/en_US/assets/downloads/pdf/summaryofprop.pdf
82. Rousche, P.J., Pellinen, D.S., Pivin, D.P., Williams, J.C., Vetter, R.J., and Kipke, D.R.: Flexible Polyimide-based Intracortical Electrode Arrays with Bioactive Capability. IEEE Trans. In Biomedical Engineering **48**(3), 361–371 (2001)
83. Owens, A.L., Denison, T.J., Versnel, H., Rebbert, M., Peckerar, M., and Shamma, S.A.: Multielectrode Array for Measuring Evoked Potentials from Surface of Ferret Primary Auditory Cortex. J. Neuroscience Methods **58**(1–2), 209–220 (1995)
84. Boppart, S.A., Wheeler, B.C., and Wallace, C.S.: A Flexible Perforated Microelectrode Array for Extended Neural Recordings. IEEE Transactions on Biomedical Engineering, **39**(1), 37–42 (1992)
85. Stieglitz, T., and Meyer, J.U.: Implantable Microsystems: Polyimide-based Neuroprostheses for Interfacing Nerves. Med. Dev. Technol., **10**(6), 28–30 (1999)
86. Takeuchi, S., Suzuki, T., Mabuchi, K., and Fujita, H.: 3D Flexible Multichannel Neural Probe Array. Journal of Micromechanics and Microengineering **14**, 104–107 (2004)
87. Lee, K-K., He, J., Singh, A., Massia, S., Ehteshami, G., Kim, B., and Raupp, G.: Polyimide-based Intracortical Neural Implant with Improved Structural Stiffness. Journal of Micromechanics and Microengineering **14**, 32–37 (2004)
88. Blum, N.A., Carkhuff, B.G., Charles, Jr. H.K., Edwards, R.L., and Meyer, R.A.: Multisite Microprobes for Neural Recordings. Biomedical Engineering, IEEE Transactions on **38**, 68–74 (1991)
89. Maher, M.P., Pine, J., Wright, J., and Tai, Y.C.: The Neurochip: A New Multielectrode Device for Stimulating and Recording from Cultures Neurons. Journal of Neuroscience Methods **87**, 45–56 (1999)
90. Tooker, A., Meng, E., Ericson, J., Tai, Y.C., and Pine, J.: Biocompatible Parylene Neurocages. IEEE Engineering in Medicine and Biology Magazine **24**, 30–33 (2005)
91. Rodger, D.C., Weiland, J.D., Humayun, M.S., and Tai, Y.C.: Scalable high lead-count parylene package for retinal prostheses. Sensors and Actuators B **117**, 107–114 (2006)
92. Rodger, D.C., Fong, A.J., Li, W., Ameri, H., Lavrov, I., Zhong, H., Saati, S., Menon, P., Meng, E., Burdick, J.W., Roy, R.R., Edgerton, V.R., Weiland, J.D., Humayun, M.S. and Tai, Y.C.: High-Density Flexible Parylene-Based Multielectrode Arrays for Retinal and Spinal Cord Stimulation. Solid-State Sensors, Actuators and Microsystems Conference, 2007. TRANSDUCERS 2007. International, pp. 1385–1388 (2007)
93. Rodger, D.C., Fong, A.J., Li, W., Ameri, H., Ahuja, A.K., Guiterrez, C., Lavrov, I., Zhong, H., Menon, P., Meng, E., Burdick, J.W., Roy, R.R., Edgerton, V.R., Weiland, J.D., Humayun, M.S., and Tai, Y.C.: Flexible Parylene-Based Multielectrode Arrays for High-Density Neural Stimulation and Recording. Sensors and Actuators B **132**, 449–460 (2008)
94. Rodger, D.C., and Tai, Y.C.: Microelectronic Packaging for Retinal Prosthesis. IEEE Engineering in Medicine and Biology Magazine **24**(5), 52–57 (2005)
95. Frazier, A.B., O'Brien, D.P., and Allen, M.G.: Two dimensional metallic microelectrode arrays for extracellular stimulation and recording of neurons. Micro Electro Mechanical Systems, MEMS '93, IEEE, pp. 195–200 (1993)

96. Frazier, A.B., Ahn, C.H., and Allen, M.G.: Development of Micromachined Devices using Polyimide-based Processes. Sensors and Actuators A **45**, 47–53 (1994)
97. O'Brien, D.P., Allen, M.G., and Nichols, T.R.: Flexible Microelectrode Arrays with Integrated Insertion Devices. Annals of Biomedical Engineering **25**(sup. 1), 58 (1997)
98. O'Brien, D.P., Nichols, T.R., and Allen, M.G.: Flexible microelectrode arrays with integrated insertion devices. Micro Electro Mechanical Systems, 2001. MEMS 2001. The 14th IEEE International Conference on, pp. 216–219 (2001)
99. Rowe L., Almasri, M., Fogleman, N., Frazier, A.B., and Brewer, G.J.: An active microscaffold for culturing 3-D neuronal networks. Solid-State Sensors, Actuators and Microsystems, 2005 Digest of Technical Papers. TRANSDUCERS '05. The 13th International Conference on, pp. 948–951 (2005)
100. Rowe L., Almasri, M., Lee, K., Fogleman, N., Brewer, G.J., Nam, Y., Wheeler, B.C., Vukasinovic, J., Glezer, A., and Frazier, A.B.: Active 3-D microscaffold system with fluid perfusion for culturing in vitro neuronal networks. Lab on a Chip **7**(4), 475–482 (2007)
101. Choi, Y., Choi, S-O., Shafer, R.H., and Allen, M.G.: Highly Inclined Electrodeposited Metal Lines Using an Excimer Laser Patterning Technique. Proc. IEEE Transducers Conf. (2005). doi: 10.1109/SENSOR.2005.1497360
102. Rajaraman, S., Choi, S.O., Shafer, R.H., Ross, J.D., Vukasinovic, J., Choi, Y., DeWeerth, S.P., Glezer, A., and Allen, M.G.: Microfabrication technologies for a coupled three-dimensional microelectrode, microfluidic array. Journal of Micromechanics and Microengineering **17**(1), 163–171 (2007)
103. Choi, Y., Powers, R., Vernekar, V., Frazier, A.B., LaPlaca, M.C., and Allen, M.G.: High Aspect Ration SU-8 Structures for 3-D Culturing of Neurons. ASME International Mechanical Engineering Congress and Expo, Microelectromechanical Systems, Washington, DC, USA, 15–21 November 2003.
104. Choi Y., McClain, M.A., LaPlaca, M.C., Frazier, A.B., and Allen M.G.: Three-Dimensional MEMS Microfluidic Perfusion System for Thick Brain Slice Cultures. Biomedical Microdevices **9**(1), 15–23 (2007)
105. Rajaraman, S., Choi, S-O., McClain, M.A., Ross, J.D., LaPlaca, M.C., and Allen, M.G.: Metal Transfer Micromolded Three-Dimensional Microelectrode Arrays for in-vitro Brain Slice Recordings, IEEE Journal of Microelectromechanical Systems. **20**(2), 396–409 (2011)
106. Allen, M.G., Choi, S-O., Park, J-H., Wu, X., Zhao, Y., Yoon, Y-K., and Rajaraman, S.: Method for Making Electrically Conductive Three-Dimensional Structures. U.S. Patent Application No. 2008/0063866 A1 (2008)